

Review

Electrospun Nanofiber-Based Membranes for Water Treatment

Yixuan Tang [†], Zhengwei Cai [†] , Xiaoxia Sun, Chuanmei Chong, Xinfei Yan, Mingdi Li and Jia Xu ^{*}

Key Laboratory of Marine Chemistry Theory and Technology, Ministry of Education, College of Chemistry and Chemical Engineering, Ocean University of China, Qingdao 266100, China; yixuantang06@163.com (Y.T.); caizhengwei2021@163.com (Z.C.); sunxia0812@163.com (X.S.); 18264722913@163.com (C.C.); yanxinfei99@163.com (X.Y.); mingdili08@163.com (M.L.)

^{*} Correspondence: jiapipi2@163.com

[†] These authors contributed equally to this work.

Abstract: Water purification and water desalination via membrane technology are generally deemed as reliable supplementaries for abundant potable water. Electrospun nanofiber-based membranes (ENMs), benefitting from characteristics such as a higher specific surface area, higher porosity, lower thickness, and possession of attracted broad attention, has allowed it to evolve into a promising candidate rapidly. Here, great attention is placed on the current status of ENMs with two categories according to the roles of electrospun nanofiber layers: (i) nanofiber layer serving as a selective layer, (ii) nanofiber layer serving as supporting substrate. For the nanofiber layer's role as a selective layer, this work presents the structures and properties of conventional ENMs and mixed matrix ENMs. Fabricating parameters and adjusting approaches such as polymer and cosolvent, inorganic and organic incorporation and surface modification are demonstrated in detail. It is crucial to have a matched selective layer for nanofiber layers acting as a supporting layer. The various selective layers fabricated on the nanofiber layer are put forward in this paper. The fabrication approaches include inorganic deposition, polymer coating, and interfacial polymerization. Lastly, future perspectives and the main challenges in the field concerning the use of ENMs for water treatment are discussed. It is expected that the progress of ENMs will promote the prosperity and utilization of various industries such as water treatment, environmental protection, healthcare, and energy storage.

Keywords: electrospinning; electrospun nanofiber-based membranes (ENMs); nanofiber layer; membrane fabrication; water treatment



Citation: Tang, Y.; Cai, Z.; Sun, X.; Chong, C.; Yan, X.; Li, M.; Xu, J. Electrospun Nanofiber-Based Membranes for Water Treatment. *Polymers* **2022**, *14*, 2004. <https://doi.org/10.3390/polym14102004>

Academic Editors: Tatyana S. Sazanova, Anton Petukhov and Maxim Trubyanov

Received: 13 April 2022

Accepted: 10 May 2022

Published: 13 May 2022

Publisher's Note: MDPI stays neutral with regard to jurisdictional claims in published maps and institutional affiliations.



Copyright: © 2022 by the authors. Licensee MDPI, Basel, Switzerland. This article is an open access article distributed under the terms and conditions of the Creative Commons Attribution (CC BY) license (<https://creativecommons.org/licenses/by/4.0/>).

1. Introduction

Clean water is known as one of the essential resources for human utilization. According to a United Nations report, by 2050 nearly six billion people worldwide will suffer from clean water scarcity [1]. Numerous plants, among other things, such as municipal/industrial wastewater purification and seawater desalination, were established to ensure a sufficient clean water supply. Currently, water purification plants predominantly involve physical approaches (filtration, sedimentation, and centrifugation), chemical approaches (flocculation, coagulation, and oxidation), biological approaches (anaerobic and aerobic digestions), and reverse osmosis and flash distillation technologies, aiming at the reduction and removal of contaminants for clean potable water [2,3]. Among these techniques, membrane technology, with unique advantages of non-phase change, low energy consumption, high-quality water supply, space-saving, and easy integration with other processes, has aroused dramatic interest in academia and industry. Membrane separation processes can be classified according to separation principles and membrane properties. Based on the pressure-driven separation process, membranes can be classified as microfiltration, ultrafiltration, nanofiltration, reverse osmosis, forward osmosis, and pressurized delayed infiltration. According to the thermal-driven separation process, membranes can be divided into pervaporation and membrane distillation.

The rapid expansion of nanotechnology, such as nanomaterials with extraordinary physical and chemical properties, could assist in satisfying the demand for high-quality purification applications. The nanomaterials include zero-dimensional nanoparticles (all three dimensions are in the range of 1–100 nm, for example, quantum dots), one-dimensional materials (one of the dimensions is on a nanometer scale, examples include nanofibers, nanorods, nanotubes, nanowires), and two-dimensional nanosheets (all three dimensions are >100 nm) [4]. Among these, nanofibers, especially synthesized by electrospinning for a predominant electroactive phase, contribute extraordinary features to nanotechnology's development [5]. Nanofibers are unique among the numerous types of nanomaterials due to their remarkably high specific surface area and porosity. In general, there are many techniques to produce nanofibers, such as bicomponent extrusion, electrospinning, melt blowing, phase separation, centrifugal spinning, drawing, self-assembly, and template synthesis (Table 1). The electrospinning (ES) technique is a cost-effective, simple and economic strategy for nanofiber production with the most control over parameters of nanofibers varying in size, shape, and doping [6]. Relatively symmetrical and homogeneous-structured nanofiber scaffolds can be developed alongside the production of membranes with excellent performance in water purification operations [7]. Membranes mainly fabricated via a sole or integrated ES technique, typically known as electrospun nanofiber-based membranes (ENMs), consist of nanofiber layers with overlapped nanofibers of diameters ranging from several nanometers to a few microns. ENMs have been regarded as one of the most promising orientations for energy storage, health care, electricity generation, biotechnology, and environmental applications, benefiting from these features, especially water purification and desalination [8].

The efficiency of a membrane-based desalination system, particularly its permeability (water flux) and separation efficiency (solute rejection), depend considerably on the membrane properties and performance [9]. For increasingly enhanced separation requirements to be met, the ENMs require constant improvements and optimization for increased efficiency in both pressure-driven and thermal-driven processes with less consumption. According to our best knowledge, few studies have focused on the production and application of ENMs, with an eye to functionalized nanofibers for specific applications. As shown in Figure 1a, ENMs can be divided into the following two categories according to the roles of electrospun nanofiber layers: (i) nanofiber layer serving as a selective layer, (ii) nanofiber layer serving as supporting substrate. The synthesis method of ENMs can be classified as single polymers, mixed polymers, polymers with nanofiber, and surface modifications. ENMs mainly have the following application fields: microfiltration, ultrafiltration, nanofiltration, reverse osmosis, forward osmosis, pervaporation, membrane distillation, etc. Regarding applications in water purification and desalination, the position of the nanofiber layer in ENMs have suggested that there are two types of ENMs, with the nanofiber layer serving as a selective layer and a support substrate, respectively (Figure 1b,c). This paper will comprehensively review the latest developments, especially within the last five years of these application in water purification and desalination, alongside cutting-edge research advancements [10].

Table 1. Comparison of different fabrication techniques of fibers.

Techniques	Technical Process	Materials	Benefits	Drawbacks	Ref.
Electrospinning	<ul style="list-style-type: none"> Polymer solution or melt flow and transform into polymer jet from spinneret under a high voltage electric field (usually 6 kV above); When the jet is extended and solvent is vaporized, the nanofibers in specific dimensions are collected by collectors 	Polyester, polyamide, polyvinyl alcohol, polyacrylonitrile, polyurethane, polyp-benzoyl, p-phenylenediamine etc.	<ul style="list-style-type: none"> High-productive; Simple for operation; Products with advantages of exceedingly porous, well interconnected, huge internal surface area, three-dimensional fibrous system and extraordinarily separation ability 	<ul style="list-style-type: none"> Vulnerable mechanical strength 	[11,12]
Dry spinning	<ul style="list-style-type: none"> Polymer solution is extruded from spinneret and cooled down by hot air stream; Polymer trickles turn to fibers in solid state during solvent extraction 	Cellulose acetate, polyolefin, polyvinyl chloride, vinylidene chloride spandex etc.	<ul style="list-style-type: none"> Wide range of raw materials; Pollution-free and no solvent recovery problems 	<ul style="list-style-type: none"> Low yield 	[13,14]
Wet spinning	<ul style="list-style-type: none"> Polymer solution is extruded from spinneret and then solidified into fibers through coagulating bath; Fibers are extruded and collected 	Polyacrylonitrile, polyvinyl alcohol, polyvinyl chloride, viscose, polypyrrole, conductive polyaniline, inorganic nanofibers like carbon nanotubes etc.	<ul style="list-style-type: none"> Uniform structure and high quality of fibers; Directional fibers can be collected; Possible to produce inorganic nanofibers for separation application 	<ul style="list-style-type: none"> Low speed in spinning; Short Fibers 	[15,16]
Emulsion spinning	<ul style="list-style-type: none"> Polymer powder is dispersed in easy-spinning carrier solution; Carriers dissolve in high-temperature processing; Polymer powder is melted or sintered into successive fibers 	Polytetrafluoroethylene, ceramic, silicon carbide, monox, chloroethylene etc.	<ul style="list-style-type: none"> Specificity in the polymers unsuitable for dry spinning and wet spinning 	<ul style="list-style-type: none"> Presence of structural defects and impurities; Low structural stability; 	[17,18]
Melt spinning	<ul style="list-style-type: none"> Polymer particles are heated, melt and extruded into spinneret; Polymer jet is impinged and cooled down by hot air stream to produce fine fibers; The fine fibers are collected in a collector screen 	Polyolefin, polyamide, polyester, polyvinyl chloride etc.	<ul style="list-style-type: none"> Simplicity and efficiency; No solvent recovery problems 	<ul style="list-style-type: none"> Requirements of high voltage electric field and temperature; None nano-sized fiber 	[19,20]
Phase separation spinning	<ul style="list-style-type: none"> Polymer solution of two or multiple components is exposed to the gelation temperature to get the gel; Phase separation of solvent and polymer occur due to temperature and pressure changes; Nanofibers are generated and collected after solvent extraction and matrix drying 	Polyacrylonitrile, poly (2, 6-dimethyl p-phenyl ether), polypropylene, polyvinyl alcohol	<ul style="list-style-type: none"> Feasibility on the polymers difficult for electrospinning and melt blowing; Mass production; 	<ul style="list-style-type: none"> Limited range of polymer-solvent system; Difficult solvent recovery; Low structural stability; Rare polymers with good gelation ability 	[21,22]

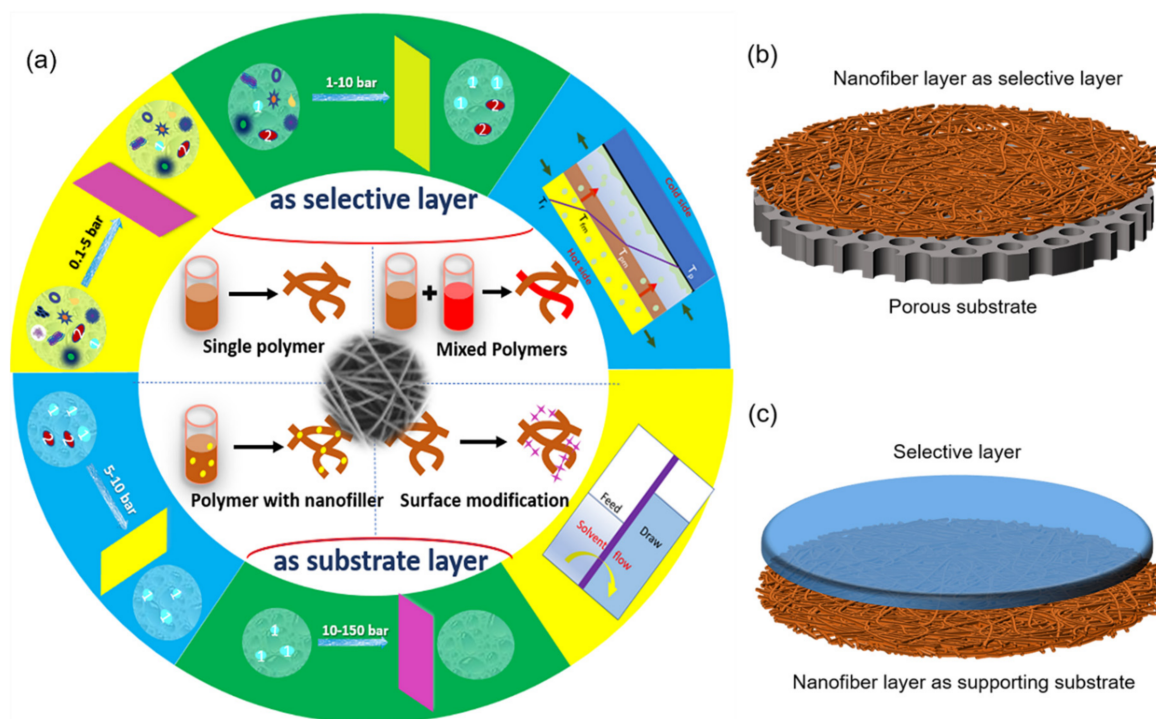


Figure 1. (a) Preparation and application of ENMs; (b,c) ENMs schematic images of two roles of nanofiber layers: served as selective layer (b) and supporting substrate (c).

2. Electrospinning Technique and Process

2.1. Electrospinning Technique

In the late 16th century, William Gilbert began to describe the behavior of magnetic fields and electrostatic phenomena. The process of ES was patented by J.F. Cooley in 1900 and by W.J. Morton in 1902. In 1934, Formalas invented an experimental apparatus for the preparation of polymer fibers by electrostatic force. The experimental device vividly reveals how polymer solutions form a fluid between electrodes. It was first time volume production of fibers in high voltage static electricity was described in detail and is now mostly recognized as the beginning of ES technology in fiber preparation. During the 1930s to 1990s, with significant attention directed towards ES exploration, many researchers applied for a series of patents. However, few succeeded. Nonetheless, given the rapid development of nanotechnology in recent years, ES technology has thrived and prospered and is once again thriving and prospering. This brings about renewed hope for this technology in scientific research, and also renews industrial circles' hopes for this technology. Throughout this period, the development of ES has undergone four stages. The first stage focused on the spinnability of different polymers, the influence of process parameters on the diameters and properties of fibers during the spinning process, and the optimization of the process parameters. The second stage concentrated on the diversity of the nanofibers and their structure. The third stage specialized in applying electrospun fiber in the fields of energy, environment, biomedicine and optoelectronics, whereas the fourth stage paid heed to the large-scale manufacturing of electrospun fibers.

ES technology has the advantages of simple manufacturing devices, low spinning costs, a wide range of spinnable materials, and precise and controllable processes [23,24]. Because of these advantages, ES technology has become one of the universal methods for the effective preparation of nanofiber materials. The electrospun nanofibers bear several remarkable properties such as a small diameter, large surface area, high aspect ratio, unique physiochemical properties, and flexibility [25]. The ES technique device consists of a high-voltage supply device, a syringe tube with small diameter needles, and a metal collecting plate/roller (Figure 2). The temperature and humidity of the environment should be

kept stable. During the ES process, a superior high voltage electrical force is utilized on the polymer-solvent system (polymer solution or polymer melt). After that, the polymer solution is injected from the spinneret by overcoming surface tension of the solution under a superior high electric field force. A polymer jet is principally affected by surface tension and electrostatic force during the stretching process. In this process, the stretching of fibers is affected by various forces such as surface tension, Coulomb repulsion force, electrostatic force viscoelasticity, gravity, and air resistance [26]. Subsequently, collectors collect a strip of fiber in a specific dimension when the jet is stretched, and the solvent evaporates through the air. During the ES process, the bending instability results in the high stretching of the fiber.

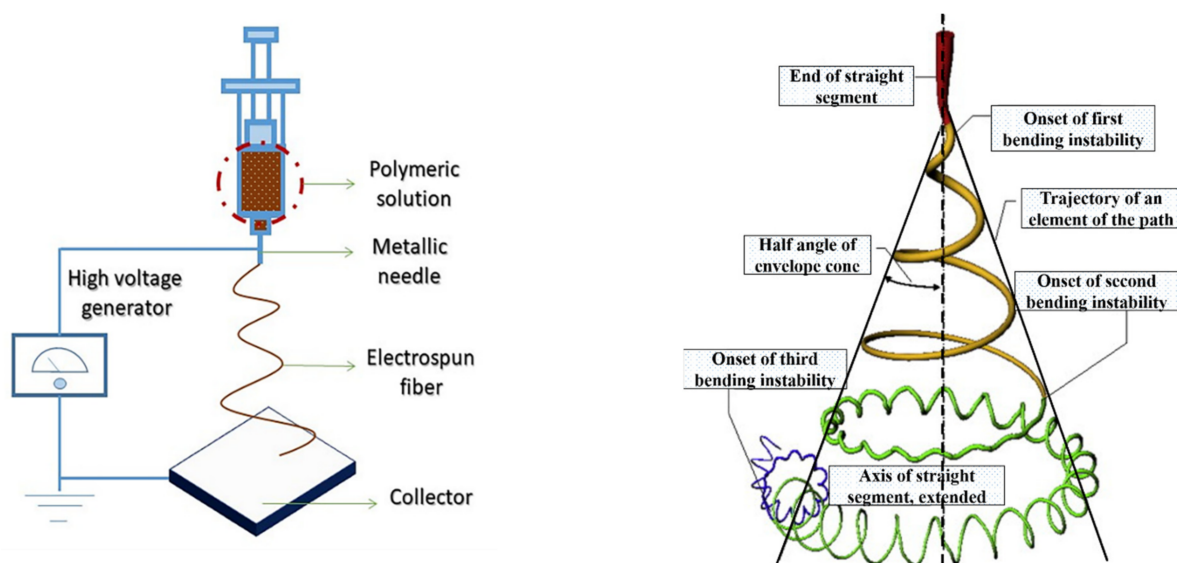


Figure 2. Schematic representation of the ES process. Reprinted with permission from Ref. [27]. 2020, Elsevier.

2.2. Effects of Electrospinning Parameters

Nanofibers with variable dimensions or morphologies can be manufactured under different ES conditions [28,29]. The polymer fiber diameter and morphology are affected by both the polymeric solution properties as well as the process parameters. The main factors influencing the polymer solution properties include polymer weight and architecture, solution concentration, polymer viscosity, solution conductivity, and surface tension and solvent. Operating parameters include electric potential, polymer solution flow rate, the distance between the capillary and collector, needle gauge, collector, ambient temperature, humidity, and air velocity in the chamber. The relationship between surface properties and ES parameters is listed in Table 2.

Table 2. Effects of different conditions on the nanofibers in electrospinning technique.

Sorts	Factors	Influences	Ref.
Polymer solution	Concentration	<ul style="list-style-type: none"> • Viscosity and surface tension of polymer solution increase as the concentration increases; • Diameters and pore sizes of nanofibers increase as the solution concentration increases; • Instable nanofibers with a low linear density are produced by polymer solution at a low concentration 	[30,31]
	Polymer molecular structure	<ul style="list-style-type: none"> • Smoother surfaces and a larger diameter are caused by a branched polymer compared with the linear polymer; • Bead-free structures are manufactured by linear polymers 	[32,33]

Table 2. Cont.

Sorts	Factors	Influences	Ref.
	Polymer molecular weight	<ul style="list-style-type: none"> Smoothness of nanofibers is increased as the polymer molecular weight increases 	[34,35]
	Viscosity	<ul style="list-style-type: none"> Diameters and pore sizes of nanofibers increase as the polymer viscosity increases; The production of nanofibers is directly influenced 	[36,37]
	Conductivity	<ul style="list-style-type: none"> Diameters decrease and pore sizes increase as the conductivity increases; Bead-formed fibers are caused by a higher conductivity 	[38,39]
	Surface tension	<ul style="list-style-type: none"> Diameters decrease and pore sizes increase as the surface tension increases; Impurities are hard to avoid when surfactants are utilized to reduce the tension 	[40,41]
	Solvent volatility	<ul style="list-style-type: none"> Wet fiber, molten fiber, or even negligible fiber collection are the result of solvent volatility; Highly volatile solutions may result in intermittent spinning due to polymer solidification at the tip of the spinneret; A proper solvent can make the produced fiber uniform and stable 	[42,43]
Fabrication conditions	Electric potential	<ul style="list-style-type: none"> Larger and faster tensile of the solution droplets as the voltage increases; Droplet splitting ability is enhanced, leading to a larger diameter of nanofibers 	[44,45]
	Flow rate of polymer solution	<ul style="list-style-type: none"> Diameters and the beads of nanofibers increase with the higher flow rate; Pore sizes vary due to the different flow rate 	[46,47]
	Distance between spinneret and collector	<ul style="list-style-type: none"> Diameters of nanofibers reduce with the larger distance; Beads appear and the products turn unstable on account of the larger distance 	[48,49]
	Syringe Needle gauge	<ul style="list-style-type: none"> Diameters increase and pore sizes decrease as the nozzle diameter increases; Productivity is enhanced by the smaller diameter of the needle 	[50,51]
	Collector	<ul style="list-style-type: none"> Flat, cylindrical, and prismatic collectors are popular 	
Ambient conditions	Temperature	<ul style="list-style-type: none"> Solvent volatilization and nanofiber solidification are accelerated by the increase in temperature; Electrical stretching of the fluid jet is early terminated by temperature increases; The instability of nanofibers is enhanced due to the decrease in solution viscosity and surface tension by temperature increases 	[52,53]
	Humidity	<ul style="list-style-type: none"> Thinner, less sticky and bead-formed structures are caused by the higher humidity, as well as larger diameters and pore sizes 	[54,55]
	Air velocity in the chamber	<ul style="list-style-type: none"> Nanofibers are enabled to be collected on the collector layer by layer when increasing air flow rate, consistent with the spinning direction; Instability in the ES process is caused by the increased velocity of cross flow air 	[56,57]

3. ENMs with a Nanofiber Layer as the Selective Layer

ENMs with a controllable fiber diameter and pore size, narrow pore size distribution, high and tunable porosity, low tortuosity, and controllable thickness—as well as a customized structure—have drawn great attention from researchers and the industrial purification field. The parameters of the ES process, such as the concentration of the polymeric solution, solvents ratio, applied electric voltage, the ambient temperature, and so

forth, have been proved to necessitate critical optimization. One polymer (or co-blended polymers) with inorganic additives to fabricate ENMs is commonly utilized in the water purification. Modification and variations are further required to provide versatile physico-chemical properties and better performance in the water desalination process. Herein, the influencing factors, such as electrospinning conditions, mixed matrix solution, and surface modification, are discussed.

3.1. Conventional ENMs

Polyacrylonitrile (PAN) [58], polysulfone (PSF), polyvinylidene fluoride (PVDF) [59], polyurethane (PU) [60], polyvinyl alcohol (PVA) [61], polyethersulfone (PES) [62], fluoropolymer, poly(vinylidene fluoride-co-hexafluoropropylene) (PVDF-co-HFP, PH), polystyrene (PS) [63], and polydimethylsiloxane (PDMS) [64] are favored for their adjustable fiber diameters, impressive membrane porosities and uniform pore sizes [65]. It is a universal preference that these polymers be electrospun into ENMs with the pore size range of 0.1–1.0 μm , which significantly affects the removal of particles exceeding 1.0 μm . These membranes can be regulated under different operating conditions to enhance the performance of ENMs.

3.1.1. Polymer Blending

The selection of polymers will affect the parameters, such as surface tension, electrical conductivity, and viscosity of the ES solution [66]. ES needs to overcome the solution surface tension for spinning, and reducing the surface tension facilitates the formation of fibers without beads. Too low a viscosity may lead to the interruption of polymer filaments and polymer droplets, while too high a viscosity makes it difficult to extrude the polymer. The polymer solution conductivity affects the fiber diameter. The choosing of the appropriate one or mix of the polymer solutions significantly affects the properties of ENMs.

ENMs with different properties are required for various applications, and ENMs prepared from a single polymer make it difficult to meet the demand. In terms of co-blending polymers, ES is a technique to combine polymers with different properties into one reservoir, electrospun together to improve the performance of the membranes [67]. The nanofibers made of a polymer blend can also give rise to new applications due to the integration of functions originating from individual components. Silk (SF) has excellent mechanical and binding resistance properties. Poly(ethyleneimine) (PEI) is a hyperbranched cationic polymer which was shown earlier to improve the antibacterial activity of resins. Ugur et al. [68] combined SF, PEI, and PMMA with ES technology to successfully prepare antibacterial- and mechanically enhanced nanofiber membranes.

The coexistence of phenol and salt in wastewater increases its toxicity and has a detrimental effect on the ecosystem. Therefore, it is necessary to prepare a membrane that is highly permeable to phenol and impermeable to water and salt to treat phenol-laden saline wastewater. PDMS, as a superhydrophobic material with a low surface energy and surface density, is widely used to improve membrane hydrophobicity. However, simple methods for the preparation of superhydrophobic PDMS membranes are still to be explored. Ren et al. [68,69] used poly(methyl methacrylate) (PMMA) as a carrier polymer for superhydrophobic ENMs to creatively fabricate PDMS/PMMA ENMs to treat phenol-laden saline wastewater. The result showed that an increase in PDMS/PMMA mass ratio led to a rise of solution viscosity, where the cosolvent was composed of equal volumes of DMF and THF. The optimized membrane exhibited a high WCA of $\sim 163^\circ$, a good permeation flux of $\sim 39.6 \text{ L m}^{-2} \text{ h}^{-1}$ and an excellent salt rejection of $\sim 99.96\%$.

Zhang et al. [70] incorporated polyaniline (PANi) into styrene block copolymer polystyrene-*b*-(ethylene-co-butene)-*b*-styrene (SEBS) dissolved solution for SBES/PANi ENMs, which accordingly obtained excellent strain recovery capability and thermal stability compared with the pristine SEBS ENMs. The SEBS/PANi ENMs had a remarkable corrosion resistance to stainless steel, even under large tensile deformation. Zhu et al. [71] newly developed

Janus fibrous membranes by incorporating $\text{NH}_3 \cdot \text{H}_2\text{O}$, 17-FAS, and PVDF powder into PVA/PAA solutions to fabricate PVA/PAA ENMs (Figure 3a,b). When the simulated hypersaline wastewater composed of 3.5 wt% of NaCl, 0.1 g of SDBS and 1.0 g of lubricating oil was desalinated, a high water flux of over $27 \text{ Lm}^{-2}\text{h}^{-1}$ and a high desalination efficiency of $\sim 100\%$ were achieved after heat treatment.

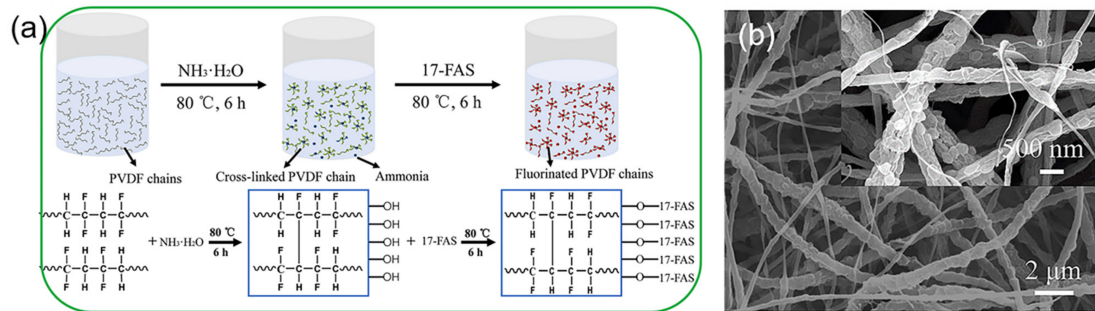


Figure 3. (a) Schematic illustration of PVDF chains crosslinking induced by $\text{NH}_3 \cdot \text{H}_2\text{O}$ and the 17-FAS grafting onto PVDF polymer chains; (b) FE-SEM images of PVDF ENMs through a fluorinated, self-roughened process and thermal treatment. Reprinted with permission from Ref. [72]. 2020, Elsevier.

3.1.2. Other Fabricating Parameters

As illustrated in Table 2, operating conditions consequently worked effectively on nanofibers and ENMs. The polymer solution (such as volume and concentration) and operating parameters (such as temperature and pH) are explored separately to improve the performance of the nanofiber layer.

Attia et al. [73] fabricated superhydrophobic dual-layer PVDF ENMs with different membrane thicknesses by varying the volume and concentration of the polymer solution (Figure 4). The multiple heavy metal rejection of the prepared ENMs was all above 99%. Moreover, dual-layer PVDF ENMs possessed a higher permeate flux above $23 \text{ Lm}^{-2}\text{h}^{-1}$ for 2500 ppm total heavy metal concentrations and exhibited a mechanical performance and a slight reduction in LEP compared with the single-layer ENMs in the same volume of polymer solution by air-gap membrane distillation.

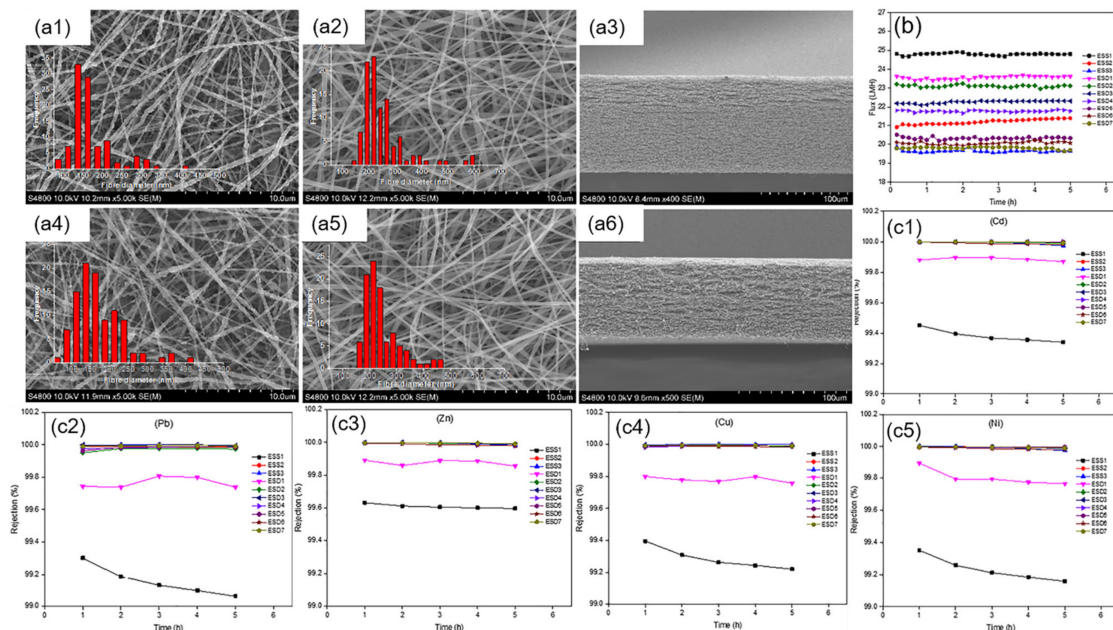


Figure 4. (a) SEM images for the top layer (a1,a4), bottom layer (a2,a5), and cross-section (a3,a6) of the prepared PVDF ENMs; (b) Permeate flux of PVDF ENMs (ESD1–7); (c) Rejection of Cd, Pb, Zn, Cu and Ni (c1–c5). Reprinted with permission from Ref. [73]. 2018, Elsevier.

Wang et al. [74] first adjusted the membrane porosity using a facile hot-pressing method. The membrane porosity decreases from ~86% to ~34% after the hot-pressing process, increasing the rejection of 0.2 μm particles from 0 to 100%. Compared to conventional microfiltration media, these membranes possessed a high flux value of $\sim 10,320 \text{ Lm}^{-2}\text{h}^{-1}\text{MPa}^{-1}$ and low degrees of fouling in the long run. Barroso-Solares et al. [75] reported a post-pressing on neat PMMA fibers before utilizing water-in-oil emulsion separation for homogeneous distribution. In addition, flexible pH is also the critical point at which to adjust the surface morphologies of ENMs. Shekarabi et al. [76] studied the pH effect on PAN ENMs with an aluminum precursor added in spinning solution, based on an ionization topic and a metallic chemical structure for fast heavy metal ions adsorption. Electrostatic excretion between Cr^{6+} and membrane surface was raised, with the pH values increasing from 3.5 to 11. Hence, the adsorption was negligible until it reached a pH value of 11, and Cr^{6+} was adsorbed notably and was precipitated at pH 3.5 by taking place on the solid surface.

3.2. Mixed Matrix ENMs

Recently, the fabrication of mixed matrix membranes with dispersive nanoparticles incorporated into the continuous polymer matrix is gaining importance for its advantages compared with polymeric and inorganic membranes. Preparation of the mixed matrix nanofiber selective layer by incorporating inorganic nanomaterials, organic crosslinking agent, and carbon-based nanomaterials into polymer solution to improve the ENMs performance are illustrated below [77].

3.2.1. Inorganic Metal Incorporation

Inorganic metal modification consists of metal nanoparticles (Ag, Fe) and metal oxide materials (Al_2O_3 , TiO_2 , MOFs) [78]. Morphologies and structures of the composite mixed matrix ENMs are altered, hence varying from that of the original. This generates excellent water purification efficiency in heavy metal ions adsorption, organic dyes removal, antibacterial applications, oil–water separation, and some membrane distillation processes.

Ag nanoparticles of dimensions ranging from several nanometers to tens of nanometers, with their excellent properties of killing and inhibiting bacteria and microorganisms [79], have sparked great interest in mixed matrix electrospun selective layer formation in membrane production for water desalination [80]. However, when directly added to the polymer solution, Ag nanoparticles will agglomerate, and hardly disperse on the electrospun nanofibers. Therefore, the reduction reaction between Ag^+ and Ag nanoparticles is selected to solve this problem. Yuan et al. [81] added Ag^+ into the PVA solution and heated it to 150 $^\circ\text{C}$ to make the obtained PVA ENMs composite insoluble in water. The Ag^+ was reduced by PVA, amalgamated together and simultaneously modified on the membrane mat with the ES process. The optimum adsorption performance of the obtained ENMs towards Hg^{2+} in water was $\sim 248 \text{ mg/g}$ in 333 K.

In addition to metal ions, metal compounds such as Al_2O_3 and TiO_2 are widely used for incorporation into polymer solutions. Attia et al. [82] fabricated hydrophobic PVDF/ Al_2O_3 ENMs through a one-step production. Superhydrophobic Al_2O_3 nanoparticles functionalized by branched hydrocarbon were firstly incorporated into polymer solution to facilitate hydrophobicity and surface roughness. Cationic surfactant HTAB was used to reduce the beads of fibers. The WCA was about 150° , higher than the pure PVDF membrane's temperature of 132° (Figure 5a,b). The synthesized membranes were advantageous compared to commercial membranes, where the heavy metal rejection was up to 99.4%, with a permeate flux of about $20 \text{ Lm}^{-2}\text{h}^{-1}$. Their group [83] then combined electrospray with an electrospinning technique to fabricate superhydrophobic PVDF/ Al_2O_3 ENMs with beaded surface features (Figure 5c,d). The synthesized membrane possessed a superior permeating performance of $\sim 18.6 \text{ Lm}^{-2}\text{h}^{-1}$ and $\sim 99.99\%$ rejection of multiple heavy metal elements, with high liquid entry pressure, water contact angle and a low sliding angle.

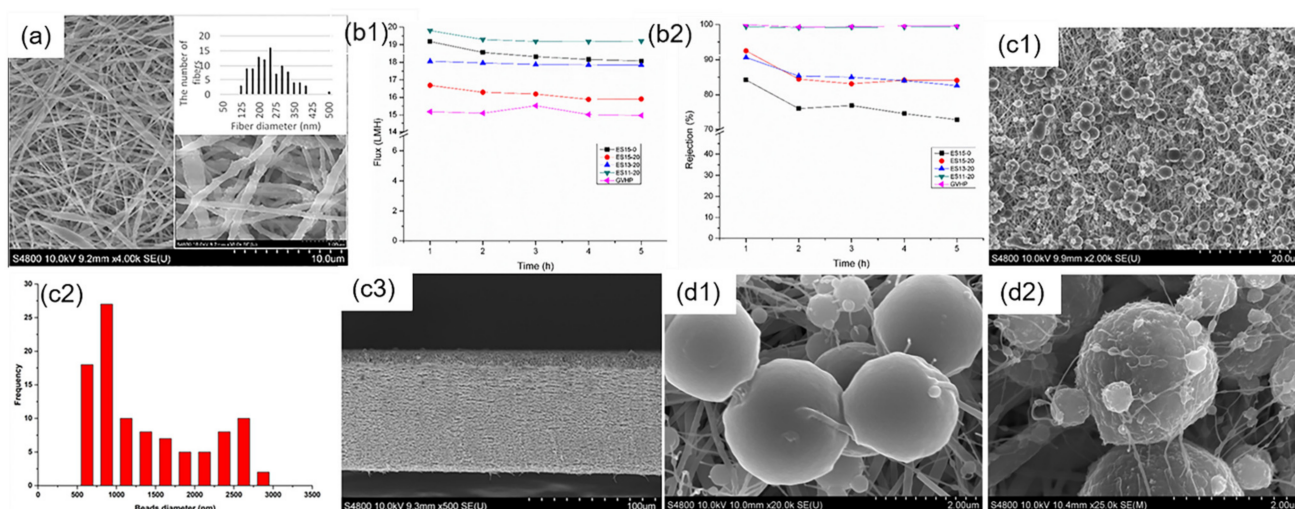


Figure 5. (a) SEM images of optimized fibers; (b1,b2) Flux data and rejection percentage as a function of time for the commercial and the synthesized membranes; Reprinted with permission from Ref. [82]. 2017, Elsevier. (c1–c3) SEM images of top surface, beads diameter and cross-section of the optimized PVDF/Al₂O₃ ENMs; (d1,d2) SEM images of beads without and with 30 wt% Al₂O₃ nanoparticles. Reprinted with permission from Ref. [83]. 2018, Elsevier.

TiO₂ has also attracted much attention as it can improve the hydrophilicity of nanofibers, accelerate the interaction between water and membranes, and even has abilities to inhibit certain bacteria. Razzaz et al. [84] fabricated the chitosan/TiO₂ ENMs by TiO₂ incorporated into chitosan dissolved in 3% acetic acid solution. Controlling the concentration of TiO₂ nanoparticles was essential for the obtainment of uniform and non-defect membranes. As the 2 wt% TiO₂ nanoparticles were mixed with 7 wt% chitosan, agglomeration and coagulation could not occur in the structure of the composite ENMs, which increased the adsorption sites of the membrane. At a pH level of 6, the maximum adsorption capacities for Cu²⁺ and Pb²⁺ ions of the composite ENMs were ~710.3 and ~579.1 mg/g, respectively. This was due to the electrostatic interaction between the heavy metal ions and nanofibers. Besides, the addition of zeolite to the nanofibers enhanced the adsorption capacities towards heavy metal ions [85].

3.2.2. Inorganic Nonmetal Incorporation

Inorganic nonmetallic nanomaterials such as SiO₂ [86], carbon nanotubes (CNTs), zeolite [87,88], graphene, and graphene oxide (GO) were incorporated into the polymeric solution for functional improvements.

Silica nanoparticles added to the polymer solution have the ability to improve the mechanical strength of nanofibers, increase the glass transition temperature of ENMs, and prevent the appearance of beads throughout the ES process [89,90]. Hou et al. [91] dissolved the polyvinylidene fluoride-co-hexafluoropropylene (PVDF-HFP) in a cosolvent of DMF/acetone, and added SiO₂ emulsion into the reagent to obtain PVDF-HFP/SiO₂ ENMs. With the mass ratio of SiO₂ increasing, though the membrane porosity decreased gradually, the pores shrunk while the thickness of membranes was enhanced, resulting in the improvement of salt rejection efficiency. The WCA was over 150°, owing to the rougher hydrophobic surface. The highest permeate flux was up to 48.6 kg/m²h and the rejection of NaCl was maintained at nearly 100% after 240 h of continuous operation of the membrane distillation process.

CNT membranes are expected to be used as high-performance self-assembly membranes in water purification, and their molecular sieving performance mainly depends on the effective pore size of the membranes [92]. CNTs in polymer composites can enhance the tensile modulus and strength of polymers, which are immobilized in nanofibers by ES to enhance the mechanical toughness of the composite nanofibers [93]. Excellent mechanical

strength and modulus are attributed to the strong electrostatic attraction between electropositive CNT nanotubes and negative polymer matrix. The robust composite nanofiber membrane is promising for water purification processes. CNTs and its modified versions are considered ideal nanofillers because of their high thermal and mechanical stability and their light weight. Yan et al. [94] prepared a hierarchical carbon nanofiber membrane by electrospinning PAN/TPA solution, followed by pre-oxidation and carbonization, to achieve high-performance desalination under sunlight, even in acid/alkali conditions. The ENMs performed well in interfacial solar desalination of $1.36 \text{ kgm}^{-2}\text{h}^{-1}$ evaporation rate and $>99.9\%$ rejection of main ions in seawater with markedly improved surface roughness and surface wettability.

The idea of using industrial waste materials (that might pollute the environment) to make composite membranes for water treatment may bring a new impetus to the field. Fly ash, as a relatively abundant and inexpensive adsorbent, has attracted a lot of attention in the field of water treatment. It can be used to adsorb different toxic substances, such as arsenic, dyes, volatile organic compounds, and many more [95,96]. Pant et al. [97] prepared a stable silver-doped fly ash/polyurea (Ag-FA/PU) nanocomposite multifunctional film using fly ash particles (FAPs) through a simple one-step ES process. Colloidal solution of PU with FAPs and Ag metal precursor was used to fabricate nanocomposite spider-web-like membrane using an ES process. The films can be used for adsorptive removal of dyes and arsenic, destructive removal of microorganisms, and removal of particulate impurities by single membrane filtration using a continuous filtration process.

Graphene and GO possess most of the properties of carbon nanotubes. Their exceptional chemical and thermal stability and rich hydrophilic functional groups contribute to their being attractive nanofillers [98,99]. Woo et al. [100] incorporated graphene into a PH solution and fabricated the superhydrophobic PH/graphene ENMs. As 5 wt% graphene was added, the porosity reached $\sim 88\%$ and WCA was up to $\sim 162^\circ$. Graphene in the nanofibers increased the roughness of the membrane surface, thereby affecting high surface hydrophobicity, and thermal and chemical stability additionally in the 60 h membrane distillation operation. The composite ENMs showed a high water flux at $\sim 22.9 \text{ Lm}^{-2}\text{h}^{-1}$ and maintained a high salt rejection of $\sim 100\%$. Ahmadi et al. [101] prepared a novel electrospun nanofiber membrane by ES using sulfonated polyvinylidene fluoride (S-PVDF)/PVDF and S-PVDF/PVDF/graphene oxide (GO) with negative charge as raw materials (Figure 6). WCA of the optimized ENMs was as low as 77.1° and high purity water flux was $\sim 1222 \text{ Lm}^{-2}\text{h}^{-1}$. The irreversible fouling was controlled by enhanced hydrophilicity under 41% and the water flux recovery ratio was about 59%.

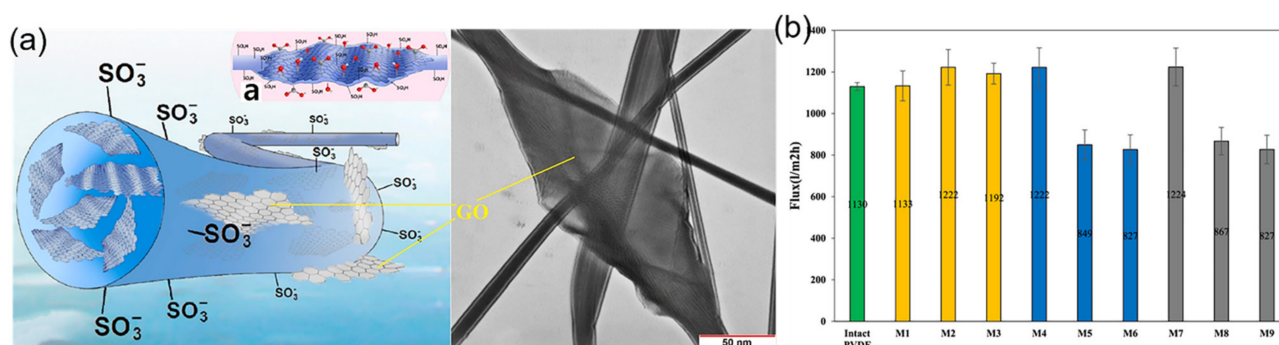


Figure 6. (a) Schematic diagrams and TEM images of S-PVDF/PVDF/GO nanofibers; (b) Water flux of PVDF ENMs with CNTs in different concentrations. Reprinted with permission from Ref. [101], 2017, Elsevier.

The shape and porosity of nanofiber membranes are crucial in water filtration. The use of spider web morphology nanofibers or nanoweb fibers in the field of water filtration has garnered considerable attention in recent years. Pant et al. [97] prepared spider-web-like silver-doped fly ash/polyurea (Ag-FA/PU) nanocomposite membranes by an ES process.

The spider-web-like nano-meeting structure enhances the adsorption of carcinogenic arsenic (As) and toxic organic dyes, as well as improves antimicrobial performance to reduce the bio-fouling of membrane filters. Inspired by a natural spider-web-like structure, Xing et al. [102] prepared a new type of atrazine molecularly imprinted nanofibrous membrane (A-MNM). The spider-web-like structure provided sufficient surface area for the formation of imprint recognition sites. Interestingly, during the separation, the target molecules are captured by the A-MNMs, just like a spider web entangles its prey in nature. The spider-web-like morphology nanofibers or nano-net fibers further broadens the application of ENMs in the field of water purification.

3.2.3. Organic Incorporation

In contrast to various inorganic additives, there are fewer applications of organic additives due to various rigorous conditionalities, which, in general, are covalent organic frameworks (COFs), metal organic frameworks (MOFs), poly-cyclodextrin [103,104], β -cyclodextrin, and their modifiers [105].

MOFs are a class of nanoporous materials composed of central metal clusters or ions and organic ligands, which possess a large specific surface area, a high porosity, a low thermal conductivity, and ordered nanopores [106]. In recent years, MOFs have attracted significant interest for their role as nanofillers in pressure-driven liquid separations to drastically improve separation performances by providing additional water channels [107]. In 2016, Zuo and Chung first introduced MOFs into membranes for membrane distillation, which led to a breakthrough in new applications for ENMs [108]. Shooto et al. [109] discovered that the diameter of PVA nanofibers decreased when the content of MOFs increased. This subsequently contributed to the increase of solution conductivity by MOFs. The prepared PVA/MOFs ENMs exhibited a higher uptake capacity of Pb^{2+} in aqueous solution over commonly used activated carbon. Efome et al. [110] dispersed pre-hydrated Zr-based MOF-808 (Zr-MOF-808) in PAN solution for PAN/Zr-MOF-808 ENMs. Zr-based MOF-808 was synthesized and hydrated according to Li et al. [111] in 2015 with the mechanism of electrostatic interaction and metal ions binding to adsorption sites on MOFs. The obtained ENMs showed optimized adsorption capacities of ~ 225.1 mg/g and ~ 287.1 mg/g for Cd^{2+} and Zn^{2+} respectively. In the same year, they [112] added Fe-based MOF-808 into PAN solutions similarly to form PAN/Fe-MOF-808 ENMs. The synthesized ENMs can dispose ~ 395 mL of the 100 ppb Pb^{2+} solution, while maintaining adsorption capacity of above 90% for Pb^{2+} after 4 cycles.

COFs are a class of robust two- or three-dimensional extended network materials known for their artistic structures and for their potential for a wide range of applications [113,114]. Wang et al. [115] combined a new type of COF-SCU1 (firstly reported by Sichuan University [116]) with PAN powder to form a DMF solvent for electrospinning, thereby obtaining PAN/COF-SCU1 ENMs. The composite PAN/COF-SCU1 ENMs retained the strong adsorption of COFs and prevented the breakdown from pure COFs as adsorbents. The optimized adsorption of tetracycline antibiotics was above 84–99% in a neutral aqueous environment, which was far more than the 10% of pure PAN ENMs, and declined lower than 30% after five continuous cycles.

3.3. Surface Modification

The internal structure of the membrane, created by the random accumulation of nanofibers as well as surface modification, can affect both pore size and liquid entry pressure. A surge of composite ENMs with a modified nanofiber layer via organic grafting of additional functional groups has attracted great interest to achieve a higher separation performance.

Wang et al. [117] grafted hyperbranched polyethylenimine (HPEI) and glycidol onto PAA ENMs to form PAA/HPEI-glycidol ENMs via the reaction between the carboxylic group on PAA with the amine groups in HPEI, followed by the ring-opening of amine terminal groups with glycidol. The formation of the complexation compound formed boron and hydroxyl groups in glycidol, which vastly improved boron adsorption. The

maximum boron adsorption capacity of the optimized ENMs achieved up to 5.7 mmol/g and remained approximately 94% after 10 operation cycles. Zhao et al. [118] demonstrated a facile preparation of branched polyethylenimine (bPEI) grafted PAN ENMs with a refluxing approach facilitating the reaction between cyano groups of PAN and bPEI. It has been proven that the modified PAN/bPEI ENMs gained notable improvements in the adsorption of Cr^{6+} by achieving up to 637.5 mg/g, making it superior to many other adsorbents. The resulting membrane could cause the concentration of Cr^{6+} in water to drop to the WHO standard, below 0.05 mg/g, indicating its significant use in removing toxic metal ions.

Distinct methods of pre-treatment, taking the vapor activation method as an example, have been newly developed. It has been demonstrated that the surface properties were labile when exposed to organic solvents or high humidity [119]. Wu et al. [120] fluorinated PVDF/PH ENMs without surface activation via vapor deposition to lower the surface energy of the membrane (Figure 7). It was understood that, as compared with traditional dip-coating, vapor deposition is more convenient in large-scale fabrication. The optimal fluorinated ENMs showed robust anti-wetting properties during membrane distillation in the trial. Moreover, Liu et al. [121] used the solvent vapor to partially melt CA/PVDF ENMs and promoted contact points among the nanofibers for physical crosslinking, which was testified to be simple yet effective to enhance the mechanical strength of the resulting membranes.

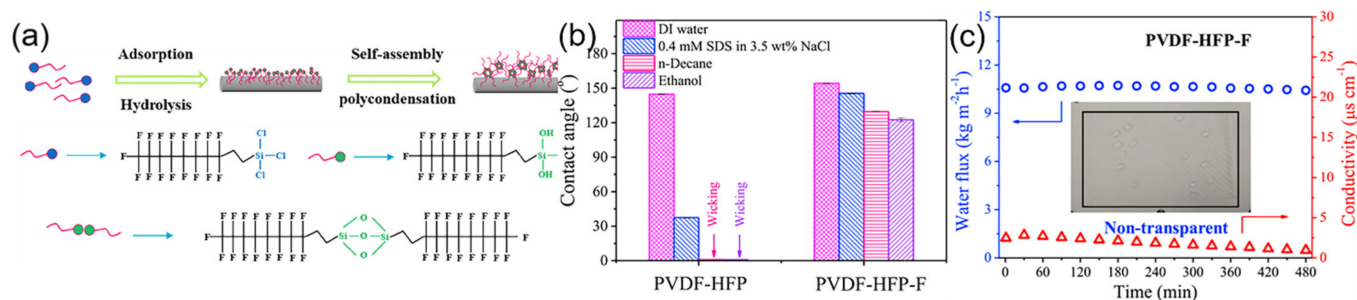


Figure 7. (a) Schematic illustration of vapor deposition fluorination; (b) Contact angles of DI water and other liquids on PVDF-HFP and PVDF-HFP-F membranes; (c) Conductivity and water flux verses time of the PVDF-HFP-F membrane in DCMD. Reprinted with permission from Ref. [120], 2020, Elsevier.

4. ENMs with Nanofiber Layer as Supporting Substrates

The nanofiber layer can also be used as the supporting substrate of ENMs, owing to its unique advantages of a good surface-to-volume ratio and splendid porosity conducive to the selective layer's growth [122]. A selective layer was generally formed on the nanofiber layer by secondary-electrospinning, inorganic deposition, polymer coating, and interfacial polymerization, which are crucial in determining the path of fluid flow and separation efficiency [123]. Moreover, structure matching, such as thickness and porosities of the supporting layer and the selective layer, should be precisely tailored by independent adjustment to achieve the best performance for the intended application.

4.1. With the Selective Layer via Secondary-Electrospinning

Dual-layer hydrophobic composite ENMs with two kinds of nanofiber layers were superior candidates in the water desalination process, especially membrane distillation, owing to its unique advantages of well-connected inner pores and low mass transfer resistance. It was reported that dual-layer ENMs, generally composed of hydrophobic/hydrophilic or superhydrophobic/less hydrophobic layers, exhibit better performance in membrane distillation than single-layer hydrophobic ENMs of the same thickness [124,125]. Besides, using a hydrophobic/hydrophilic dual-layer hollow fiber membrane for long-term DCMD operation demonstrated fewer pore wetting issues [126,127].

Woo et al. [126] prepared dual-layer ENMs composed of hydrophobic polyvinylidene fluoride-co-hexafluoropropylene (PH) top nanofiber layer with different supporting hydrophilic nanofiber layers for distillation desalination (Figure 8a–c). The heat-pressed PH/nylon-6 exhibited high hydrophobicity and enhanced mechanical and thermal properties. Large porosity (~85.3%) promoted a high flux of $\sim 15.5 \text{ Lm}^{-2}\text{h}^{-1}$ and salt rejection above 99%. An et al. [128] assembled the PH nanofiber layer and PET microfiber layer via convectional electrospinning to fabricate hierarchical composite PET/PH ENMs (Figure 8b–e). During membrane distillation, the highly hydrophobic PH nanofibers presented an enhanced anti-wetting property as well as a high salt rejection. Concurrently, PET microfibers provided an improved mass transfer and heat insulation. The relatively high permeability ($\sim 65.9 \text{ Lm}^{-2}\text{h}^{-1}$) and high salt rejection ($>99.99\%$) were optimized for the composition and thickness of membranes. Khayet et al. [129] assembled the hydrophobic bottom layer PVDF and hydrophilic top layer PSF nanofibers via electrospinning at different times successively to prepare dual-layer ENMs (Figure 8f–h). The prepared PVDF/PSF ENMs exhibited an excellent desalination performance with a flux of $\sim 53.60 \text{ Lm}^{-2}\text{h}^{-1}$, and an NaCl rejection of $\sim 99.99\%$, which is visibly higher than the traditional ENMs reported in direct contact membrane distillation. Moreover, Hou et al. [130] fabricated biomimetic PTFE/PVA ENMs via sol-gel and electrospinning methods for anti-oil-fouling membrane distillation. Their asymmetric wettability attributed by the hydrophobic PTFE nanofiber layer as the bottom layer and the highly hydrophilic PVA-Si-GA layer as the top layer, helped to sustain a stable operation over 50 h with 1000 mg/L crude oil as foulant.

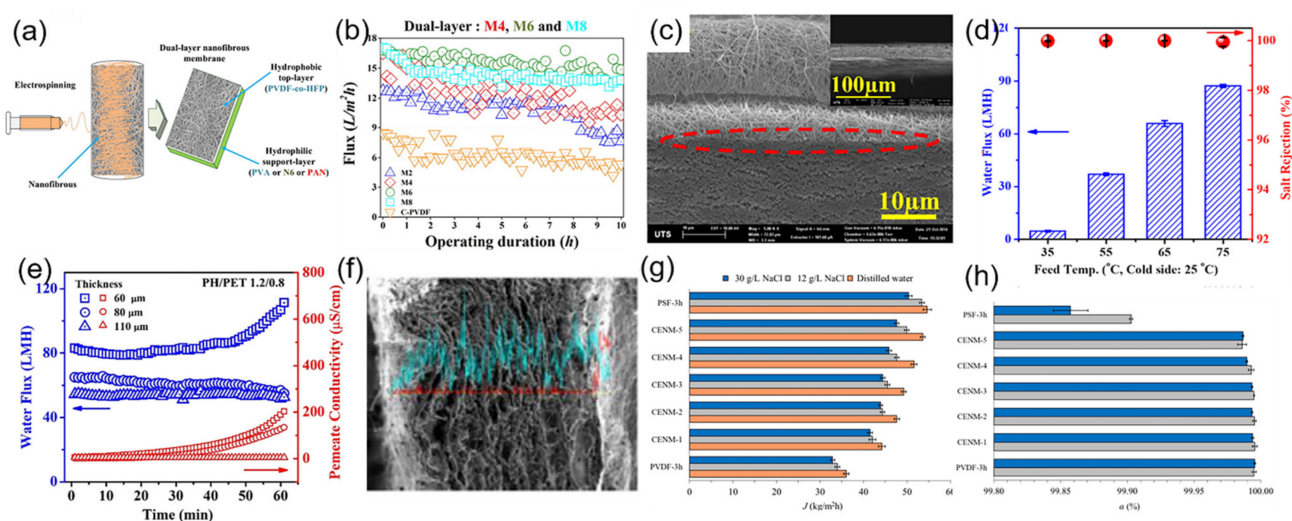


Figure 8. (a) Schematic diagram of the fabrication process of dual-layer ENMs; (b) permeance performance of the prepared ENMs; Reprinted with permission from Ref. [126]. 2017, Elsevier. (c) cross section SEM images of the optimized dual-layer ENMs; (d,e) permeating performance and stability test in different conditions of thermal and strain; Reprinted with permission from Ref. [128]. 2020, Elsevier. (f) cross-section SEM images and EDX analysis of the optimized dual-layer ENMs (CENM-5); (g,h) permeating performance of dual-layer ENMs. Reprinted with permission from Ref. [129]. 2017, Elsevier.

4.2. With the Selective Layer via Inorganic Deposition

ENMs obtained with the selective layer via inorganic deposition from the nanofiber layer can usually enhance membranes' thermodynamic and chemical stability. Properties of such hierarchical membranes are strongly affected by the selectivity of nanomaterials, which are commonly applied to heavy metals, some toxic ions adsorption and oil–water separation [131].

Yan et al. [132] coated CNT layers onto the PVDF ENMs by the heat-pressing process. The CNTs were dispersed in ethanol to spray without agglomeration. The prepared superhydrophobic PVDF/CNT ENMs exhibited the highest water flux of $\sim 28.4 \text{ Lm}^{-2}\text{h}^{-1}$, with

above 26 h of steady performance in a vacuum membrane distillation. Jiang et al. [133] deposited hydrophobic single-side CNTs on the hydrophilic PAN nanofiber layer through a vacuum filtration process in order to fabricate Janus PAN/CNTs ENMs. Various concentrations of the PAN and CNT solution generated different properties of hydrophobicity/hydrophilicity in both sides of the membrane (Figure 9). The optimized oil rejection was increased to exceed 99.5% followed by the incorporation of CNTs with a high flux of $\sim 120,000 \text{ Lm}^{-2}\text{h}^{-1}\text{MPa}^{-1}$.

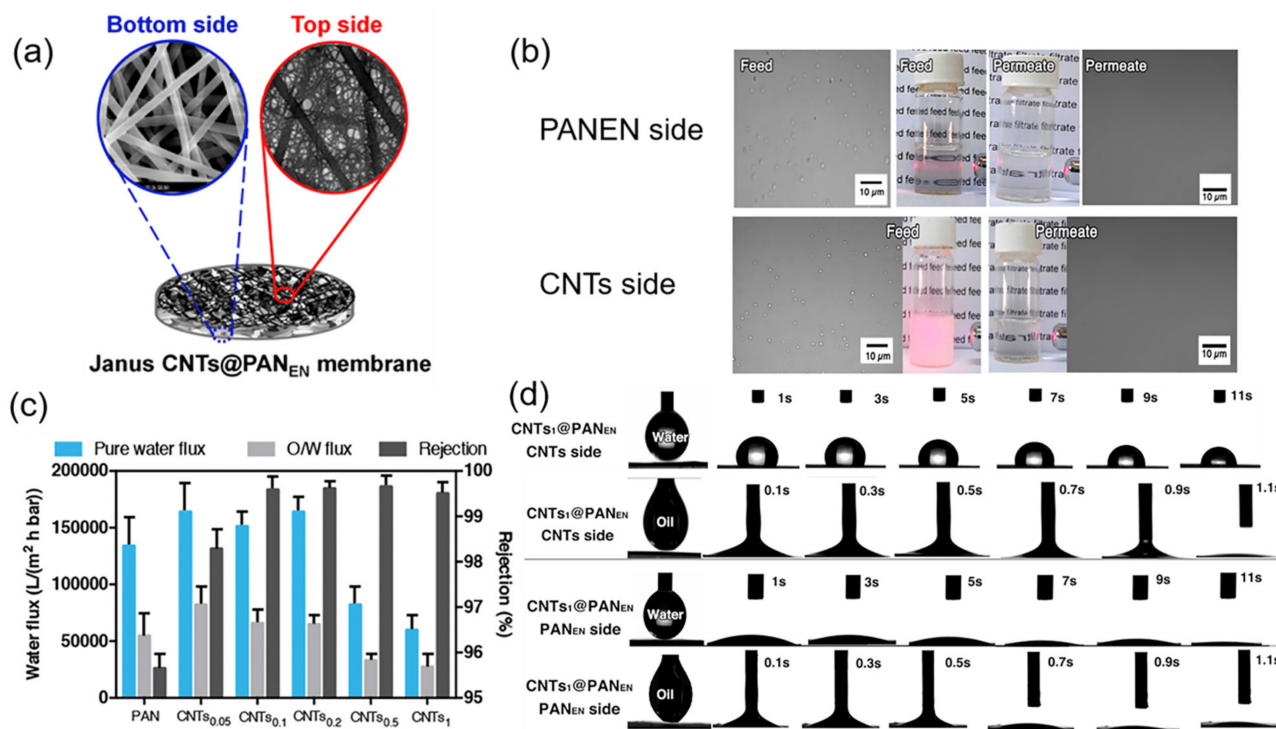


Figure 9. (a) Schematic illustration and SEM images of Janus PAN/CNTs ENMs; (b) separation results by two sides of Janus PAN/CNTs_{0.5} ENMs; (c) pure water flux, O/W flux and water rejection by the pure PAN and PAN/CNTs ENMs; (d) spreading behaviors of water and oil droplet on two sides of PAN/CNTs_{0.5} ENMs. Reprinted with permission from Ref. [133]. 2017, Elsevier.

Electrospray technique, an electrostatic atomization process, is utilized for the beaded fiber structure without compromising pore architecture or structural integrity [134]. Guo et al. [135] fabricated superhydrophobic PVDF-co-HFP ENMs with monolayer nanofiber and nanospheres by one-step biaxial electrospinning and an electrospray method. Nanospheres were dispersed uniformly on each nanofiber by electrospraying. Huang et al. [136] used the electrospraying technique on chitosan-rectorite nanospheres from the aminated PAN (APAN) nanofiber layer via shoulder-to-shoulder electrospinning. The aminating modification was carried on the surface of PAN by DETA. Chitosan was extruded into nanospheres by electrospray and was assembled on APAN nanofibers to enlarge the inner three-dimensional space and to facilitate the water flux with the resulting undermined flow resistance. With visible improvements seen among the amine groups in APAN regarding the adsorption process, the APAN-CA ENMs exhibited at least a double increment during the adsorption process towards Pb^{2+} in contrast to the original PAN-CS membranes.

4.3. With the Selective Layer via Polymer Coating

Various materials, such as chitosan [137], PES [138], DETA, PVA [139], and PDMS [140], with or without nanoparticles such as TiO_2 incorporated, were coated as selective layers on the surface of nanofiber layers, forming new types of ENMs to be applied in ultrafiltration and oil–water separation processes specifically [141].

Zhao et al. [142] coated amino-rich hydrothermal DETA onto the PAN nanofiber layer after an efficient hydrothermal carbonization method. Amino groups of DETA available reacted with the carboxyl groups of the carbonaceous PAN nanofiber layer to form an amide bond. The adsorption capacity of polluting Cr^{6+} and 2,4-dichlorophenoxyacetic acid were ~ 290.7 mg/g and ~ 164.5 mg/g, respectively, which were superior to the pure PAN ENMs. Ren et al. [143] coated TiO_2 precursor sol on the surface of the electrospun PVDF basis for improvements in hydrophobicity and pore structure of the membrane surface. The TiO_2 precursor sol was obtained from ethanol, 2,4-pentanedione, perchloric acid, and titanium (IV) isopropoxide mixtures, subsequently modified by fluoride. The resultant properties of high hydrophobicity ($\sim 157.1^\circ$), considerable wetting resistance of under 0.15 MPa, a well-distributed pore size of $0.8 \mu\text{m}$, a reasonable surface porosity of $\sim 57\%$, and a modest membrane thickness of $55 \mu\text{m}$ made the modified PVDF ENMs a competitive alternative option for DCMMD. Besides, Vanangamudi et al. [144] conducted a study by coating 18 wt% PVDF onto the hydrophilic nylon-6,6/chitosan nanofiber layer to form the Janus membrane. High hydrophilicity was created due to the intermolecular hydrogen bonding interaction between the membrane surface and water molecule, reaching the highest water permeance $\sim 5420 \text{ Lm}^{-2}\text{h}^{-1}\text{MPa}^{-1}$. Levels above 93% BSA were rejected for permeation through the membrane with decreased pore sizes at $\sim 3930 \text{ Lm}^{-2}\text{h}^{-1}\text{MPa}^{-1}$ liquid flux in the filtration process.

4.4. With the Selective Layer via Interfacial Polymerization

Besides deposition and coating, selective layers prepared via interfacial polymerization (IP) can also be formed on the surface of nanofiber layers to fabricate ENMs, which are mainly used for osmosis and nanofiltration processes. The typical material of this selective layer is polyamide (PA), which is prepared through the reaction of polyamines and acyl chloride [145].

In the forward osmosis process, Tian et al. [146] post-covered PA layer from M-phenylenediamine (MPD) and 1,3,5-trimesoylchloride (TMC) on the PET/PVA nanofiber layer that is formed from electrospinning. The diffusive resistance was primarily decreased due to the low tortuosity and inner interconnected pores in the nanofibrous support layer. These open pore structures and high roughness facilitated the water molecules to move across the membrane. The optimal water flux of 0.5 M NaCl solution was $\sim 30.6 \text{ Lm}^{-2}\text{h}^{-1}$ in the forward osmosis process. Shokrollahzadeh et al. [147] fabricated a PA rejection layer on the top surface of the PSF/PAN nanofiber layer based on the IP reaction between MPD and TMC monomers. Due to the high porosity of about 84.3% and a large number of interconnected pores in the membrane, the structural parameters were optimized to facilitate the formation of the uniform PA layer, decrease the internal concentration polarization (ICP) effect, and reverse the salt flux through the desalination. High porosity promoted the mass transfer across the membrane to allow the water flux to reach $\sim 38 \text{ Lm}^{-2}\text{h}^{-1}$ towards the NaCl solution in the forward osmosis process, which was superior to the utilization of the traditional substrate, fabricated by phase inversion. Park et al. [148] deposited the PA layer from MPD and TMC on the hydrophilic pretreated PVDF/PVA nanofiber layer (Figure 10), with the nanofibers being relatively rough and full of nano-sized pores. The PVDF/PVA nanofiber layer not only enhanced the hydrophilicity towards the liquid, but also reduced the ICP effect and reverse salt flux in the osmosis process. With 0.5 M NaCl as the draw solution and DI water as the feed solution, the water flux could reach up to $34.2 \text{ Lm}^{-2}\text{h}^{-1}$ and the reversed salt flux was as low as 0.13 g/L.

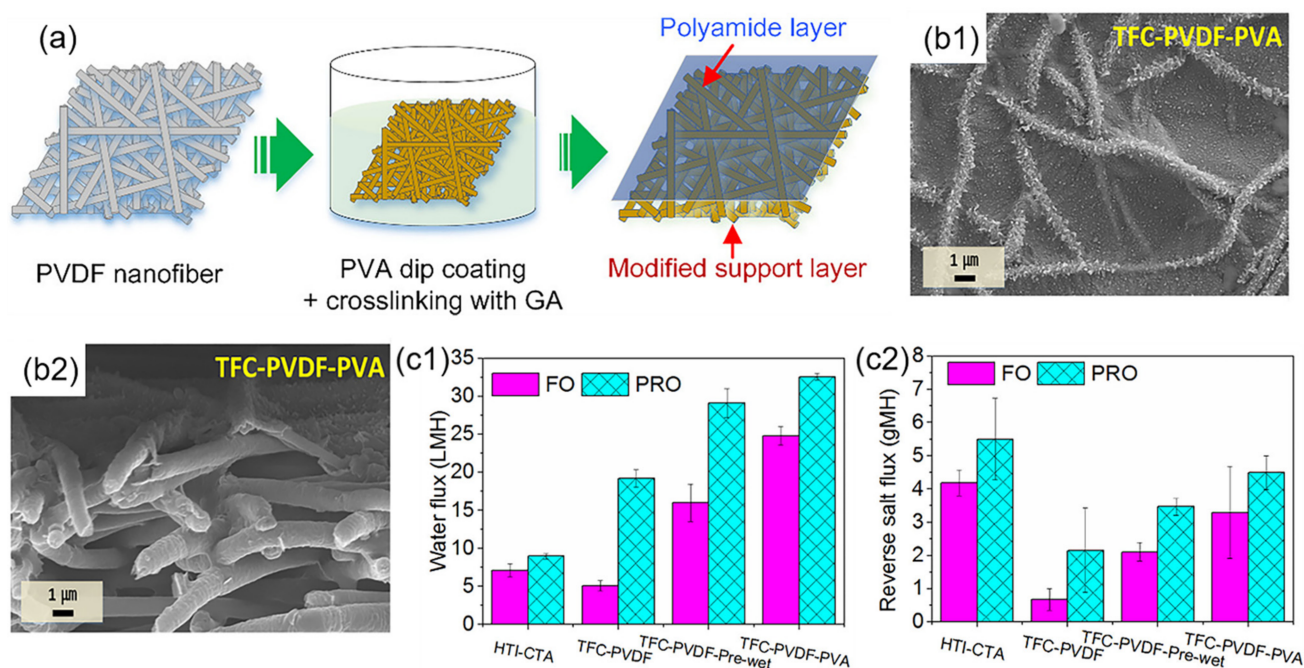


Figure 10. (a) Schematic diagram of TFN C PVDF/PVA ENMs; (b) FESEM images of PVDF/PVA nanofiber layer and TFNC PVDF/PVA ENMs for top surface (b1,b2); (c) FO performance of commercial HTI-CTA (c1) and prepared TFNC PVDF/PVA ENMs (c2). Reprinted with permission from Ref. [148]. 2017, Elsevier.

Besides, in the nanofiltration process, Mahdavi et al. [149] studied the PET nanofiber layer as substrate, p-phenylenediamine (PPD), and triethylamine (TEA) in the aqueous phase, and TMC in the oil phase to fabricate PA film as the selective layer used in the nanofiltration process. The trifluoroacetic acid (TFA) and dichloromethane (DCM) were used as solvents to sculpt morphologies of PET by dissolution. With the higher ratio value of the concentration of TFA/DCM, a better electrical conductivity of the polymeric solution could be achieved, and smaller diameters of nanofibers could be obtained. This induced the unique and flat morphology of the nanofibers, as well as numerous interconnected structures throughout the mat. Thereafter, the PA selective layer was synthesized onto the surface of the PET layer. The water flux could reach $\sim 34 \text{ Lm}^{-2}\text{h}^{-1}$ in 0.5 MPa, which is four times higher than other conventional nanofiltration membranes, while the rejection of Na_2SO_4 was about 93%. In addition, Kaur et al. [150] studied two interfacial polymerization methods onto the PVDF nanofiber layer. These two methods subsequently led to different surface topologies and different osmotic selectivity. In the first method, PVDF nanofiber layers were immersed in the aqueous and organic phases in succession. In method B, however, the order was reversed. Compared with the first method, ENMs prepared by the second method had a more uniform PA layer with a rejection rate of $\sim 80.7\%$ and a flux of $\sim 0.5 \text{ Lm}^{-2}\text{h}^{-1}$ for 2000 ppm MgSO_4 under 0.5 MPa.

5. Future Scope

Although advancements in academic research and certain applications have been reported in the field of ENMs for water treatment, there are still challenges to be confronted.

As to the electrospinning process, appropriate conditions for electrospinning and modifications are required for better manufactures and performance. Nanomaterials that are cheap, non-toxic and environmentally friendly are being focused upon. Moreover, the preparation approaches of ENMs are generally reported to be time-consuming and to have a low yield on the lab-scale. Therefore, it is necessary to build more efficient equipment for the mass production of high-quality ENMs.

As to ENM fabrication, mechanical stability, wettability and nanoscale selectivity are imperative parameters for efficient performance in water treatment. The internal bonding force in nanofibers and covalent bonding between nano-layers have considerable attention paid to them, especially in dual-layer composite ENMs, which consequently hampers the structural stability. Once the exfoliation occurs, ENMs were out of action immediately and thus lost both permeability and selectivity. Mixing matrix electrospinning solutions was proven to be a practical strategy to improve ENMs properties, and more explorations of new dopants are required for better performance as well; however, there are still problems of uniform distribution of particles in the polymer structure (agglomeration phenomenon of nanoparticles), cavity formation, immiscibility of blending polymers, and weak interactions between particles with the polymer matrix and the construction of mixed matrix membranes. Specifically, the physical and chemical stability of mixed-matrix membranes in water, including nanoparticles' detachment from the membrane surface and the incompatibility between nanoparticles and the organic polymer matrix, should be taken into account when developing new nanomaterials.

As to the operation and filtration of the membrane, durable stability, mechanical stability, and operational sustainability in realistic conditions should be crucially evaluated in the long term. The majority of reported ENMs were tested in a laboratory-simulated water environment in the short term, however, which differed from the complex water environment in realistic application. Efficient separation to complex systems with different physical and chemical properties remains to be desired and must urgently be explored; it cannot be simply resolved by ENMs yet. In addition, there is still a lack of industrial production equipment. Though certain applications were carried out in some reports, most of the promising applications are still limited to the laboratory or to the primary stage of development. More attention should be paid to the transformation of theoretical innovation into practical production.

Furthermore, the interaction between actual contaminants and ENMs should be clearly understood so that various membrane technologies can be applied extensively. It is necessary to further study the manufacture of ENMs with thin, robust, and highly selective active layers and recycling stability on the actual industrial scale.

6. Conclusions

Decent and reliable technology for water purification is urgently needed throughout the world. ENMs, with their unique features and well-organized architecture, display an up-and-coming prospect of future adsorption and filtration systems to efficiently exclude pollutants and macro/small molecules in water purification.

In this review, the current status and application aspects of traditional ES techniques are well-illustrated, with special attention on the effects of operating parameters on nanofibers for reference. ENMs, with the nanofiber layers serving as selective layers, are mainly produced in three ways: conventional ENMs, mixed matrix ENMs, and surface modification via grafting. For the production of mixed matrix electrospinning solutions, inorganic nanomaterials and organic materials are both furnished by some examples which play different roles in bacterial inhibition, dye removal, separation of oil/water systems, and so on. Such hierarchical membranes' efficiency is apparently improved by various modifiers, nanoparticles, cross-linked organic reagents, and active biopolymers. However, nanofibers' direct work as a selective layer has a relatively limited scope of utilization in low-pressure driven process like ultrafiltration, and microfiltration, as well as in thermal-driven process like membrane distillation, due to its poor mechanical strength. Therefore, typical nanofiber layers like PAN, PVDF, and PSF nanofibers and so on are widely installed as a supporting substrate, fixed with an additional skin layer by inorganic deposition, polymer coating, and interfacial polymerization to meet the demand of water treatment in different conditions. All of these contribute to the separation performances of organic pollutants, heavy metals, and antifouling performance in water treatment. It is considered

that the ENM market has enormous potential for further development and is anticipated to boom in the immediate future for water purification.

Author Contributions: Y.T., Z.C. and J.X. contributed the central idea, analyzed most of the data, and wrote the initial draft of the paper; X.S. and C.C. contributed to refining the ideas and carried out additional analyses and finalizing of this paper; X.Y. and M.L. contributed to literature and manuscript editing. All authors have read and agreed to the published version of the manuscript.

Funding: This work was supported by NSFC (No. 21878279), Natural science fund of Shandong Province Project (No. ZR2018MB032).

Institutional Review Board Statement: Not applicable.

Informed Consent Statement: Not applicable.

Data Availability Statement: Not applicable.

Conflicts of Interest: The authors declare no conflict of interest.

References

1. Celik, A.; Baker, R.; Arslan, Z. Highly efficient, rapid, and concurrent removal of toxic heavy metals by the novel 2D hybrid LDH-[Sn₂S₆]. *Chem. Eng. J.* **2021**, *426*, 131696–131709. [[CrossRef](#)]
2. Giwa, A.; Hasan, S.W. Novel thermosiphon-powered reverse osmosis: Techno-Economic Model for Renewable Energy and Fresh Water Recovery. *Desalination* **2018**, *435*, 152–160. [[CrossRef](#)]
3. Ullah, A.; Shahzada, K.; Khan, S.W.; Starov, V. Purification of produced water using oscillatory membrane filtration. *Desalination* **2020**, *491*, 114428. [[CrossRef](#)]
4. Saleem, H.; Trabzon, L.; Ali, K.; Zaidia, S.J. Recent advances in nanofibrous membranes Production and applications in water treatment and desalination. *Desalination* **2020**, *478*, 114178. [[CrossRef](#)]
5. Orudzhev, F.; Ramazanov, S.; Sobola, D. Ultrasound and water flow driven piezophototronic effect in self-polarized flexible α -Fe₂O₃ containing PVDF nanofibers film for enhanced catalytic oxidation. *Nano Energy* **2021**, *90*, 106586–106599. [[CrossRef](#)]
6. Kaspar, P.; Sobola, D.; Částková, K. Case study of polyvinylidene fluoride doping by carbon nanotubes. *Materials* **2021**, *14*, 1428. [[CrossRef](#)] [[PubMed](#)]
7. Manaf, O.; Anjana, K.; Prasanth, R.; Reshmi, C.R.; Juraij, K.; Rajesh, P.; Chingakham, C.; Sajith, V.; Sujith, A. ZnO decorated anti-bacterial electrospun ABS nanocomposite membrane for oil-water separation. *Mater. Lett.* **2019**, *256*, 126626. [[CrossRef](#)]
8. Shibuya, M.; Park, M.J.; Lim, S.; Phuntsho, S.; Matsuyama, H.; Shon, H.K. Novel CA/PVDF nanofiber supports strategically designed via coaxial electrospinning for high performance thin-film composite forward osmosis membranes for desalination. *Desalination* **2018**, *445*, 63–74. [[CrossRef](#)]
9. Huang, D.; Wu, J.; Wang, L.; Liu, X.; Meng, J.; Tang, X.; Tang, C.; Xu, J. Novel insight into adsorption and co-adsorption of heavy metal ions and an organic pollutant by magnetic graphene nanomaterials in water. *Chem. Eng. J.* **2019**, *358*, 1399–1409. [[CrossRef](#)]
10. Luo, F.; Wang, J.; Yao, Z.; Zhang, L.; Chen, H. Polydopamine nanoparticles modified nanofiber supported thin film composite membrane with enhanced adhesion strength for forward osmosis. *J. Memb. Sci.* **2021**, *618*, 118673. [[CrossRef](#)]
11. Niknejad, A.S.; Bazgir, S.; Kargari, A. Desalination by direct contact membrane distillation using a superhydrophobic nanofibrous poly (methyl methacrylate) membrane. *Desalination* **2021**, *511*, 115108. [[CrossRef](#)]
12. Liu, Y.; Gao, X.; Zhang, L.; Shen, X.; Du, X.; Dou, X.; Yuan, X. Mn₂O₃ nanoflower decorated electrospun carbon nanofibers for efficient hybrid capacitive deionization. *Desalination* **2020**, *494*, 114665. [[CrossRef](#)]
13. Yao, M.; Woo, Y.C.; Tijing, L.D.; Shim, W.-G.; Choi, J.-S.; Kim, S.-H.; Shon, H.K. Effect of heat-press conditions on electrospun membranes for desalination by direct contact membrane distillation. *Desalination* **2016**, *378*, 80–91. [[CrossRef](#)]
14. Liu, Y.; Du, X.; Wang, Z.; Zhang, L.; Chen, Q.; Wang, L.; Liu, Z.; Dou, X.; Zhu, H.; Yuan, X. MoS₂ nanoflakes-coated electrospun carbon nanofibers for “rocking-chair” capacitive deionization. *Desalination* **2021**, *520*, 115376. [[CrossRef](#)]
15. Essalhi, M.; Khayet, M.; Ismail, N.; Sundman, O.; Tavajohi, N. Improvement of nanostructured electrospun membranes for desalination by membrane distillation technology. *Desalination* **2021**, *510*, 115086. [[CrossRef](#)]
16. Zhong, D.; Zhou, J.; Wang, Y. Hollow-fiber membranes of block copolymers by melt spinning and selective swelling. *J. Memb. Sci.* **2021**, *632*, 119374. [[CrossRef](#)]
17. Cai, J.; Liu, X.; Zhao, Y.; Guo, F. Membrane desalination using surface fluorination treated electrospun polyacrylonitrile membranes with nonwoven structure and quasi-parallel fibrous structure. *Desalination* **2018**, *429*, 70–75. [[CrossRef](#)]
18. Liu, Y.; Gao, J.; Ge, Y.; Yu, S.; Liu, M.; Gao, C. A combined interfacial polymerization and in-situ sol-gel strategy to construct composite nanofiltration membrane with improved pore size distribution and anti-protein-fouling property. *J. Memb. Sci.* **2021**, *623*, 119097. [[CrossRef](#)]
19. Wu, W.; Yu, L.; Li, L.; Li, Z.; Kang, J.; Pu, S.; Chen, D.; Ma, R.; An, K.; Liu, G.; et al. Electrospun nanofiber based forward osmosis membrane using graphene oxide as substrate modifier for enhanced water flux and rejection performance. *Desalination* **2021**, *518*, 115283. [[CrossRef](#)]

20. An, X.; Liu, Z.; Hu, Y. Amphiphobic surface modification of electrospun nanofibrous membranes for anti-wetting performance in membrane distillation. *Desalination* **2018**, *432*, 23–31. [[CrossRef](#)]
21. Sequeira, R.S.; Miguel, S.P.; Cabral, C.S.D.; Moreira, A.F.; Ferreira, P.; Correia, I.J. Development of a poly(vinyl alcohol)/lysine electrospun membrane-based drug delivery system for improved skin regeneration. *Int. J. Pharm.* **2019**, *570*, 118640. [[CrossRef](#)] [[PubMed](#)]
22. Sutisna, B.; Musteata, V.; Pulido, B.; Puspasari, T.; Smilgies, D.-M.; Hadjichristidis, N.; Nunes, S.P. High flux membranes, based on self-assembled and H-bond linked triblock copolymer nanospheres. *J. Memb. Sci.* **2019**, *585*, 10–18. [[CrossRef](#)]
23. Gao, N.; Yang, J.; Wu, Y.; Yue, J.; Cao, G.; Zhang, A.; Ye, L.; Feng, Z. β -Cyclodextrin functionalized coaxially electrospun poly(vinylidene fluoride) @ polystyrene membranes with higher mechanical performance for efficient removal of phenolphthalein. *React. Funct. Polym.* **2019**, *141*, 100–111. [[CrossRef](#)]
24. Attia, H.; Osman, M.S.; Johnson, D.J.; Wright, C.; Hilal, N. Modelling of air gap membrane distillation and its application in heavy metals removal. *Desalination* **2017**, *424*, 27–36. [[CrossRef](#)]
25. Pant, B.; Park, M.; Park, S. Drug delivery applications of core-sheath nanofibers prepared by coaxial electrospinning: A Review. *Pharmaceutics* **2019**, *11*, 305. [[CrossRef](#)]
26. Wang, J.; Sun, Y.; Bi, W.; Jiang, Z.; Zhang, M.; Pang, J. High-strength corrosion resistant membranes for the separation of oil/water mixtures and immiscible oil mixtures based on PEEK. *J. Memb. Sci.* **2020**, *616*, 118418. [[CrossRef](#)]
27. Reneker, D.; Yarin, A. Electrospinning jets and polymer nanofibers. *Polymer* **2008**, *49*, 2387–2425. [[CrossRef](#)]
28. Al-Attabi, R.; Rodriguez-Andres, J.; Schütz, J.A.; Bechelany, M.; Des Ligneris, E.; Chen, X.; Kong, L.; Morsi, Y.S.; Dumée, L.F. Catalytic electrospun nano-composite membranes for virus capture and remediation. *Sep. Purif. Technol.* **2019**, *229*, 115806. [[CrossRef](#)]
29. Zahari, A.M.; Shuo, C.W.; Sathishkumar, P.; Yusoff, A.R.M.; Gu, F.L.; Buang, N.A.; Lau, W.J.; Gohari, R.J.; Yusop, Z. A reusable electrospun PVDF-PVP-MnO₂ nanocomposite membrane for bisphenol A removal from drinking water. *J. Environ. Chem. Eng.* **2018**, *6*, 5801–5811. [[CrossRef](#)]
30. Soberman, M.J.; Farnood, R.R.; Tabe, S. Functionalized powdered activated carbon electrospun nanofiber membranes for adsorption of micropollutants. *Sep. Purif. Technol.* **2020**, *253*, 117461. [[CrossRef](#)]
31. Sanaeepur, H.; Ebadi Amooghini, A.; Shirazi, M.M.A.; Pishnamazi, M.; Shirazian, S. Water desalination and ion removal using mixed matrix electrospun nanofibrous membranes: A critical review. *Desalination* **2022**, *521*, 115350. [[CrossRef](#)]
32. Zhang, M.; Ma, W.; Wu, S.; Tang, G.; Cui, J.; Zhang, Q.; Chen, F.; Xiong, R.; Huang, C. Electrospun frogspawn structured membrane for gravity-driven oil-water separation. *J. Colloid Interface Sci.* **2019**, *547*, 136–144. [[CrossRef](#)] [[PubMed](#)]
33. Ren, L.-F.; Xia, F.; Shao, J.; Zhang, X.; Li, J. Experimental investigation of the effect of electrospinning parameters on properties of superhydrophobic PDMS/PMMA membrane and its application in membrane distillation. *Desalination* **2017**, *404*, 155–166. [[CrossRef](#)]
34. Mankanjuola, O.; Janajreh, I.; Hashaikheh, R. Novel technique for fabrication of electrospun membranes with high hydrophobicity retention. *Desalination* **2018**, *436*, 98–106. [[CrossRef](#)]
35. Li, Z.; Cheng, B.; Ju, J.; Kang, W.; Liu, Y. Development of a novel multi-scale structured superhydrophobic nanofiber membrane with enhanced thermal efficiency and high flux for membrane distillation. *Desalination* **2021**, *501*, 114834. [[CrossRef](#)]
36. Yuan, Q.; Fu, Z.; Wang, Y.; Chen, W.; Wu, X.; Gong, X.; Zhen, D.; Jian, X.; He, G. Coaxial electrospun sulfonated poly(ether ether ketone) proton exchange membrane for conductivity-strength balance. *J. Memb. Sci.* **2020**, *595*, 117516. [[CrossRef](#)]
37. Yu, S.; Huang, Q.; Cheng, J.; Huang, Y.; Xiao, C. Pore structure optimization of electrospun PTFE nanofiber membrane and its application in membrane emulsification. *Sep. Purif. Technol.* **2020**, *251*, 117297. [[CrossRef](#)]
38. Hezarjaribi, M.; Bakeri, G.; Sillanpää, M.; Chaichi, M.J.; Akbari, S. Novel adsorptive membrane through embedding thiol-functionalized hydrous manganese oxide into PVC electrospun nanofiber for dynamic removal of Cu(II) and Ni(II) ions from aqueous solution. *J. Water Process. Eng.* **2020**, *37*, 101401. [[CrossRef](#)]
39. Ying, T.; Su, J.; Jiang, Y.; Ke, Q.; Xu, H. A pre-wetting induced superhydrophilic/superlipophilic micro-patterned electrospun membrane with self-cleaning property for on-demand emulsified oily wastewater separation. *J. Hazard Mater.* **2020**, *384*, 121475. [[CrossRef](#)]
40. Ghafari, R.; Scaffaro, R.; Maio, A.; Gulino, E.F.; Lo Re, G.; Jonoobi, M. Processing-structure-property relationships of electrospun PLA-PEO membranes reinforced with enzymatic cellulose nanofibers. *Polym. Test.* **2020**, *81*, 106182. [[CrossRef](#)]
41. Kebria, M.R.S.; Rahimpour, A.; Salestan, S.K.; Seyedpour, S.F.; Jafari, A.; Banisheykholeslami, F.; Tavajohi Hassan Kiadeh, N. Hyper-branched dendritic structure modified PVDF electrospun membranes for air gap membrane distillation. *Desalination* **2020**, *479*, 114307. [[CrossRef](#)]
42. Cui, J.; Li, F.; Wang, Y.; Zhang, Q.; Ma, W.; Huang, C. Electrospun nanofiber membranes for wastewater treatment applications. *Sep. Purif. Technol.* **2020**, *250*, 117116. [[CrossRef](#)]
43. Liu, H.-C.; Wang, H.-X.; Yang, Y.; Ye, Z.-Y.; Kuroda, K.; Hou, L.-a. In situ assembly of PB/SiO₂ composite PVDF membrane for selective removal of trace radiocesium from aqueous environment. *Sep. Purif. Technol.* **2021**, *254*, 117557. [[CrossRef](#)]
44. Chen, S.; Xie, Y.; Chinnappan, A.; Wei, Z.; Gu, Q.; He, H.; Fang, Y.; Zhang, X.; Lakshminarayanan, R.; Zhao, W.; et al. A self-cleaning zwitterionic nanofibrous membrane for highly efficient oil-in-water separation. *Sci. Total Environ.* **2020**, *729*, 138876. [[CrossRef](#)]

45. Hou, D.; Ding, C.; Fu, C.; Wang, D.; Zhao, C.; Wang, J. Electrospun nanofibrous omniphobic membrane for anti-surfactant-wetting membrane distillation desalination. *Desalination* **2019**, *468*, 138876. [[CrossRef](#)]
46. Xu, G.-R.; An, X.-C.; Das, R.; Xu, K.; Xing, Y.-L.; Hu, Y.X. Application of electrospun nanofibrous amphiphobic membrane using low-cost poly (ethylene terephthalate) for robust membrane distillation. *J. Water Process. Eng.* **2020**, *36*, 114068. [[CrossRef](#)]
47. Guo, X.; Gao, H.; Wang, S.; Yin, L.; Dai, Y. Scalable, flexible and reusable graphene oxide-functionalized electrospun nanofibrous membrane for solar photothermal desalination. *Desalination* **2020**, *488*, 114535. [[CrossRef](#)]
48. Wang, Y.; Xu, J.; Shen, Y.; Wang, C.-a.; Zhang, Z.; Li, F.; Cheng, J.; Ye, Y.; Shen, R. Fabrication of energetic aluminum core/hydrophobic shell nanofibers via coaxial electrospinning. *Chem. Eng. J.* **2022**, *427*, 132001. [[CrossRef](#)]
49. Guo, J.; Deka, B.J.; Kim, K.-J.; An, A.K. Regeneration of superhydrophobic TiO₂ electrospun membranes in seawater desalination by water flushing in membrane distillation. *Desalination* **2019**, *468*, 114054. [[CrossRef](#)]
50. Huang, A.; Liu, F.; Cui, Z.; Wang, H.; Song, X.; Geng, L.; Wang, H.; Peng, X. Novel PTFE/CNT composite nanofiber membranes with enhanced mechanical, crystalline, conductive, and dielectric properties fabricated by emulsion electrospinning and sintering. *Compos. Sci. Technol.* **2021**, *214*, 108980. [[CrossRef](#)]
51. Tai, Y.; Yang, S.; Yu, S.; Banerjee, A.; Myung, N.V.; Nam, J. Modulation of piezoelectric properties in electrospun PLLA nanofibers for application-specific self-powered stem cell culture platforms. *Nano Energy* **2021**, *89*, 106444. [[CrossRef](#)]
52. Qin, D.; Zhang, R.; Cao, B.; Li, P. Fabrication of high-performance composite membranes based on hierarchically structured electrospun nanofiber substrates for pervaporation desalination. *J. Memb. Sci.* **2021**, *638*, 119672. [[CrossRef](#)]
53. Voniatis, C.; Barczikai, D.; Gyulai, G.; Jedlovszky-Hajdu, A. Fabrication and characterisation of electrospun Polycaprolactone/Polysuccinimide composite meshes. *J. Mol. Liq.* **2021**, *323*, 115094. [[CrossRef](#)]
54. Mavukkandy, M.O.; Ibrahim, Y.; Almarzooqi, F.; Naddeo, V.; Karanikolos, G.N.; Alhseinat, E.; Banat, F.; Hasan, S.W. Synthesis of polydopamine coated tungsten oxide@poly(vinylidene fluoride-co-hexafluoropropylene) electrospun nanofibers as multifunctional membranes for water applications. *Chem. Eng. J.* **2022**, *427*, 131021. [[CrossRef](#)]
55. Khadem Modarresi, Z.; Mowla, D.; Karimi, G. Electrodialytic separation of phosphate from sewage sludge ash using electrospun ion exchange membranes. *Sep. Purif. Technol.* **2021**, *275*, 119202. [[CrossRef](#)]
56. Kim, Y.; Kim, Y.W.; Lee, S.B.; Kang, K.; Yoon, S.; Choi, D.; Park, S.H.; Jeong, J. Hepatic patch by stacking patient-specific liver progenitor cell sheets formed on multiscale electrospun fibers promotes regenerative therapy for liver injury. *Biomaterials* **2021**, *274*, 120899. [[CrossRef](#)]
57. Zhan, F.; Yan, X.; Li, J.; Sheng, F.; Li, B. Encapsulation of tangeretin in PVA/PAA crosslinking electrospun fibers by emulsion-electrospinning: Morphology characterization, slow-release, and antioxidant activity assessment. *Food Chem.* **2021**, *337*, 127763. [[CrossRef](#)]
58. Wang, Z.; Sahadevan, R.; Crandall, C.; Menkhaus, T.J.; Fong, H. Hot-pressed PAN/PVDF hybrid electrospun nanofiber membranes for ultrafiltration. *J. Memb. Sci.* **2020**, *611*, 118327. [[CrossRef](#)]
59. Li, Z.; Liu, Y.; Yan, J.; Wang, K.; Xie, B.; Hu, Y.; Kang, W.; Cheng, B. Electrospun polyvinylidene fluoride/fluorinated acrylate copolymer tree-like nanofiber membrane with high flux and salt rejection ratio for direct contact membrane distillation. *Desalination* **2019**, *466*, 68–76. [[CrossRef](#)]
60. Ghorai, S.K.; Roy, T.; Maji, S.; Guha Ray, P.; Sarkar, K.; Dutta, A.; De, A.; Bandyopadhyay, S.; Dhara, S.; Chattopadhyay, S. A judicious approach of exploiting polyurethane-urea based electrospun nanofibrous scaffold for stimulated bone tissue regeneration through functionally nobbled nanohydroxyapatite. *Chem. Eng. J.* **2022**, *429*, 132179. [[CrossRef](#)]
61. Chailek, N.; Daranarong, D.; Punyodom, W.; Molloy, R.; Worajittiphon, P. Crosslinking assisted fabrication of ultrafine poly(vinyl alcohol)/functionalized graphene electrospun nanofibers for crystal violet adsorption. *J. Appl. Polym. Sci.* **2018**, *135*, 46318. [[CrossRef](#)]
62. Kallem, P.; Banat, F.; Yejin, L.; Choi, H. High performance nanofiber-supported thin film composite forward osmosis membranes based on continuous thermal-rolling pretreated electrospun PES/PAN blend substrates. *Chemosphere* **2020**, *261*, 127687. [[CrossRef](#)] [[PubMed](#)]
63. Apul, O.G.; Von Reitzenstein, N.H.; Schoepf, J.; Ladner, D.; Hristovski, K.D.; Westerhoff, P. Superfine powdered activated carbon incorporated into electrospun polystyrene fibers preserve adsorption capacity. *Sci. Total Environ.* **2017**, *592*, 458–464. [[CrossRef](#)]
64. Zhang, H.; Li, B.; Sun, D.; Miao, X.; Gu, Y. SiO₂-PDMS-PVDF hollow fiber membrane with high flux for vacuum membrane distillation. *Desalination* **2018**, *429*, 33–43. [[CrossRef](#)]
65. Moradi, G.; Rajabi, L.; Dabirian, F.; Zinadini, S. Biofouling alleviation and flux enhancement of electrospun PAN microfiltration membranes by embedding of para-aminobenzoate alumoxane nanoparticles. *J. Appl. Polym. Sci.* **2018**, *135*, 45738. [[CrossRef](#)]
66. Herrero, M.; Gómez, A. Vallés-Lluch, Role of Electrospinning Parameters on Poly(Lactic-co-Glycolic Acid) and Poly(Caprolactone-co-Glycolic acid). *Membranes* **2021**, *13*, 695.
67. Xue, J.; Wu, T.; Dai, Y. Electrospinning and electrospun nanofibers: Methods, Materials, and Applications. *Chem. Rev.* **2019**, *119*, 5298–5415. [[CrossRef](#)]
68. Karatepe, U.; Ozdemir, T. Improving mechanical and antibacterial properties of PMMA via polyblend electrospinning with silk fibroin and polyethyleneimine towards dental applications. *Bioact. Mater.* **2020**, *5*, 510–515. [[CrossRef](#)]
69. Ren, L.-F.; Ngo, H.H.; Bu, C.; Ge, C.; Ni, S.Q.; Shao, J.; He, Y. Novel external extractive membrane bioreactor (EMBR) using electrospun polydimethylsiloxane/polymethyl methacrylate membrane for phenol-laden saline wastewater. *Chem. Eng. J.* **2020**, *383*, 123179. [[CrossRef](#)]

70. Ren, L.F.; Adeel, M.; Li, J.; Xu, C.; Xu, Z.; Zhang, X.; Shao, J.; He, Y. Phenol separation from phenol-laden saline wastewater by membrane aromatic recovery system-like membrane contactor using superhydrophobic/organophilic electrospun PDMS/PMMA membrane. *Water Res.* **2018**, *135*, 31–43. [[CrossRef](#)]
71. Zhang, R.; Huang, K.; Zhu, M.; Chen, G.; Tang, Z.; Li, Y.; Yu, H.; Qiu, B.; Li, X. Corrosion resistance of stretchable electrospun SEBS/PANi micro-nano fiber membrane. *Eur. Polym. J.* **2020**, *123*, 109394. [[CrossRef](#)]
72. Zhu, Z.; Zhong, L.; Chen, X.; Zheng, W.; Zuo, J.; Zeng, G.; Wang, W. Monolithic and self-roughened Janus fibrous membrane with superhydrophilic/omniphobic surface for robust antifouling and antiwetting membrane distillation. *J. Memb. Sci.* **2020**, *615*, 118499. [[CrossRef](#)]
73. Attia, H.; Johnson, D.J.; Wright, C.J.; Hilal, N. Comparison between dual-layer (superhydrophobic-hydrophobic) and single superhydrophobic layer electrospun membranes for heavy metal recovery by air-gap membrane distillation. *Desalination* **2018**, *439*, 31–45. [[CrossRef](#)]
74. Wang, Z.; Crandall, C.; Sahadevan, R.; Menkhaus, T.J.; Fong, H. Microfiltration performance of electrospun nanofiber membranes with varied fiber diameters and different membrane porosities and thicknesses. *Polym. J.* **2017**, *114*, 64–72. [[CrossRef](#)]
75. Barroso-Solares, S.; Zahedi, M.G.; Pinto, J.; Nanni, G.; Fragouli, D.; Athanassiou, A. Oil removal from water–oil emulsions using magnetic nanocomposite fibrous mats. *RSC Adv.* **2016**, *6*, 71100–71107. [[CrossRef](#)]
76. Shekarabi, H.H.; Javid, A.H.; Azar, P.A.; Hasani, A.H. Comparison of fast elimination of Cr(VI) by alumina nanofiber and alumina nanoporous. *Int. J. Environ. Sci. TE.* **2017**, *14*, 803–812. [[CrossRef](#)]
77. Salahshoori, I.; Seyfaee, A.; Babapoor, A.; Neville, F.; Moreno-Atanasio, R. Evaluation of the effect of silica nanoparticles, temperature and pressure on the performance of PSF/PEG/SiO₂ mixed matrix membranes: A molecular dynamics simulation (MD) and design of experiments (DOE) study. *J. Mol. Liq.* **2021**, *333*, 115957. [[CrossRef](#)]
78. Yin, X.; Zhang, Z.; Ma, H.; Venkateswaran, S.; Hsiao, B.S. Ultra-fine electrospun nanofibrous membranes for multicomponent wastewater treatment: Filtration and adsorption. *Sep. Purif. Technol.* **2020**, *242*, 116794. [[CrossRef](#)]
79. Zhan, F.; Yan, X.; Sheng, F.; Li, B. Facile in situ synthesis of silver nanoparticles on tannic acid/zein electrospun membranes and their antibacterial, catalytic and antioxidant activities. *Food Chem.* **2020**, *330*, 127172. [[CrossRef](#)]
80. Zhang, L.; Li, L.; Wang, L.; Nie, J.; Ma, G. Multilayer electrospun nanofibrous membranes with antibacterial property for air filtration. *Appl. Surf. Sci.* **2020**, *515*, 145962. [[CrossRef](#)]
81. Yuan, C.-G.; Guo, S.; Song, J.; Huo, C.; Li, Y.; Gui, B.; Zhang, X. One-step fabrication and characterization of a poly(vinyl alcohol)/silver hybrid nanofiber mat by electrospinning for multifunctional applications. *Rsc Adv.* **2017**, *7*, 4830–4839. [[CrossRef](#)]
82. Attia, H.; Alexander, S.; Wright, C.J.; Hilal, N. Superhydrophobic electrospun membrane for heavy metals removal by air gap membrane distillation (AGMD). *Desalination* **2017**, *420*, 318–329. [[CrossRef](#)]
83. Attia, H.; Johnson, D.J.; Wright, C.J.; Hilal, N. Robust superhydrophobic electrospun membrane fabricated by combination of electrospinning and electrospraying techniques for air gap membrane distillation. *Desalination* **2018**, *446*, 70–82. [[CrossRef](#)]
84. Razzaz, A.; Ghorban, S.; Hosayni, L.; Irani, M.; Aliabadi, M. Chitosan nanofibers functionalized by TiO₂ nanoparticles for the removal of heavy metal ions. *J. Taiwan. Inst. Chem. Eng.* **2016**, *58*, 333–343. [[CrossRef](#)]
85. Ray, S.S.; Chen, S.-S.; Nguyen Cong, N.; Hung-Te, H.; Hau Thi, N.; Chang, C.-T. Poly(vinyl alcohol) incorporated with surfactant based electrospun nanofibrous layer onto polypropylene mat for improved desalination by using membrane distillation. *Desalination* **2017**, *414*, 18–27. [[CrossRef](#)]
86. Hosseini, S.A.; Vossoughi, M.; Mahmoodi, N.M.; Sadrzadeh, M. Efficient dye removal from aqueous solution by high-performance electrospun nanofibrous membranes through incorporation of SiO₂ nanoparticles. *J. Clean. Prod.* **2018**, *183*, 1197–1206. [[CrossRef](#)]
87. Habiba, U.; Afifi, A.M.; Salleh, A.; Ang, B.C. Chitosan/(polyvinyl alcohol)/zeolite electrospun composite nanofibrous membrane for adsorption of Cr⁶⁺, Fe³⁺ and Ni²⁺. *J. Hazard. Mater.* **2017**, *322*, 182–194. [[CrossRef](#)]
88. Anis, S.F.; Lalia, B.S.; Lesimple, A.; Hashaikeh, R.; Hilal, N. Electrically conductive membranes for contemporaneous dye rejection and degradation. *Chem. Eng. J.* **2022**, *428*, 131184. [[CrossRef](#)]
89. Rasekh, A.; Raisi, A. Electrospun nanofibrous polyether-block-amide membrane containing silica nanoparticles for water desalination by vacuum membrane distillation. *Sep. Purif. Technol.* **2021**, *275*, 119149. [[CrossRef](#)]
90. Zhao, R.; Li, Y.; Sun, B.; Chao, S.; Li, X.; Wang, C.; Zhu, G. Highly flexible magnesium silicate nanofibrous membranes for effective removal of methylene blue from aqueous solution. *Chem. Eng. J.* **2019**, *359*, 1603–1616. [[CrossRef](#)]
91. Hou, D.; Lin, D.; Ding, C.; Wang, D.; Wang, J. Fabrication and characterization of electrospun superhydrophobic PVDF-HFP/SiNPs hybrid membrane for membrane distillation. *Sep. Purif. Technol.* **2017**, *189*, 82–89. [[CrossRef](#)]
92. Wang, R.; Chen, J.; Chen, L.; Ye, Z.; Wu, C.; Gao, W.; Xie, L.; Ying, Y. Ultrathin and ultradense aligned carbon nanotube membranes for water purification with enhanced rejection performance. *Desalination* **2020**, *494*, 114671. [[CrossRef](#)]
93. Yang, Y.; Xu, Y.; Liu, Z.; Huang, H.; Fan, X.; Wang, Y.; Song, Y.; Song, C. Preparation and characterization of high-performance electrospun forward osmosis membrane by introducing a carbon nanotube interlayer. *J. Memb. Sci.* **2020**, *616*, 118563. [[CrossRef](#)]
94. Yan, J.; Xiao, W.; Chen, L.; Wu, Z.; Gao, J.; Xue, H. Superhydrophilic carbon nanofiber membrane with a hierarchically macro/meso porous structure for high performance solar steam generators. *Desalination* **2021**, *516*, 115224. [[CrossRef](#)]
95. Ahmaruzzaman, M.; Gupta, V.K. Application of coal fly ash in air quality management. *Ind. Eng. Chem. Res.* **2012**, *51*, 15299–15314. [[CrossRef](#)]
96. Ahmaruzzaman, M. Role of fly ash in the removal of organic pollutants from wastewater. *Energy Fuels* **2009**, *23*, 1494–1511. [[CrossRef](#)]

97. Pant, H.; Kim, H.; Joshi, M. One-step fabrication of multifunctional composite polyurethane spider-web-like nanofibrous membrane for water purification. *J. Hazard. Mater.* **2014**, *264*, 25–33. [[CrossRef](#)]
98. Chen, Y.; Zhao, X.; Ye, Z.; Chen, Y.; Lin, P. Robust seawater desalination and sewage purification enabled by the solar-thermal conversion of the Janus-type graphene oxide evaporator. *Desalination* **2022**, *522*, 115406. [[CrossRef](#)]
99. Seah, M.Q.; Lau, W.J.; Goh, P.S.; Ismail, A.F. Greener synthesis of functionalized-GO incorporated TFN NF membrane for potential recovery of saline water from salt/dye mixed solution. *Desalination* **2022**, *523*, 115403. [[CrossRef](#)]
100. Woo, Y.C.; Tijing, L.D.; Shim, W.-G.; Choi, J.-S.; Kim, S.-H.; He, T.; Drioli, E.; Shon, H.K. Water desalination using graphene-enhanced electrospun nanofiber membrane via air gap membrane distillation. *J. Memb. Sci.* **2016**, *520*, 99–110. [[CrossRef](#)]
101. Ahmadi, A.; Qanati, O.; Dorraji, M.S.S.; Rasoulifard, M.H.; Vatanpour, V. Investigation of antifouling performance a novel nanofibrous S-PVDF/PVDF and S-PVDF/PVDF/GO membranes against negatively charged oily foulants. *J. Memb. Sci.* **2017**, *536*, 86–97. [[CrossRef](#)]
102. Xing, W.; Ma, Z.; Wang, C. Novel molecular organic framework composite molecularly imprinted nanofibrous membranes with a bioinspired viscous bead structure for selective recognition and separation of atrazine. *ACS Appl. Mater. Interfaces* **2021**, *13*, 28749–28763. [[CrossRef](#)] [[PubMed](#)]
103. Celebioglu, A.; Yildiz, Z.I.; Uyar, T. Electrospun crosslinked poly-cyclodextrin nanofibers: Highly efficient molecular filtration through host-guest inclusion complexation. *Sci. Rep.* **2017**, *7*, 7369. [[CrossRef](#)] [[PubMed](#)]
104. Yao, Z.; Guo, H.; Yang, Z.; Qing, W.; Tang, C.Y. Preparation of nanocavity-contained thin film composite nanofiltration membranes with enhanced permeability and divalent to monovalent ion selectivity. *Desalination* **2018**, *445*, 115–122. [[CrossRef](#)]
105. Zhang, J.; Fang, W.; Zhang, F.; Gao, S.; Guo, Y.; Li, J.; Zhu, Y.; Zhang, Y.; Jin, J. Ultrathin microporous membrane with high oil intrusion pressure for effective oil/water separation. *J. Memb. Sci.* **2020**, *608*, 118201. [[CrossRef](#)]
106. Huang, Z.; Yang, G.; Zhang, J.; Gray, S.; Xie, Z. Dual-layer membranes with a thin film hydrophilic MOF/PVA nanocomposite for enhanced antiwetting property in membrane distillation. *Desalination* **2021**, *518*, 115268. [[CrossRef](#)]
107. Wu, X.-Q.; Mirza, N.R.; Huang, Z.; Zhang, J.; Zheng, Y.-M.; Xiang, J.; Xie, Z. Enhanced desalination performance of aluminium fumarate MOF-incorporated electrospun nanofiber membrane with bead-on-string structure for membrane distillation. *Desalination* **2021**, *520*, 115338. [[CrossRef](#)]
108. Zuo, J.; Chung, T.-S. Metal–Organic Framework-Functionalized Alumina Membranes for Vacuum Membrane Distillation. *Water* **2016**, *8*, 586. [[CrossRef](#)]
109. Shooto, N.D.; Dikio, C.W.; Wankasi, D.; Sikhwivhilu, L.M.; Mtunzi, F.M.; Dikio, E.D. Novel PVA/MOF Nanofibres: Fabrication, Evaluation and Adsorption of Lead Ions from Aqueous Solution. *Nanoscale Res. Lett.* **2016**, *11*, 414. [[CrossRef](#)]
110. Efome, J.E.; Rana, D.; Matsuura, T.; Lan, C.Q. Insight Studies on Metal–Organic Framework Nanofibrous Membrane Adsorption and Activation for Heavy Metal Ions Removal from Aqueous Solution. *ACS Appl. Mater. Inter.* **2018**, *10*, 18619–18629. [[CrossRef](#)]
111. Li, Z.-Q.; Yang, J.-C.; Sui, K.-W.; Yin, N. Facile synthesis of metal-organic framework MOF-808 for arsenic removal. *Mater. Lett.* **2015**, *160*, 412–414. [[CrossRef](#)]
112. Efome, J.E.; Rana, D.; Matsuura, T.; Lan, C.Q. Metal–organic frameworks supported on nanofibers to remove heavy metals. *J. Mater. Chem. A* **2018**, *6*, 4550–4555. [[CrossRef](#)]
113. Gonzales, R.R.; Park, M.J.; Bae, T.H.; Yang, Y.; Abdel-Wahab, A.; Phuntsho, S.; Shon, H.K. Melamine-based covalent organic framework-incorporated thin film nanocomposite membrane for enhanced osmotic power generation. *Desalination* **2019**, *459*, 10–19. [[CrossRef](#)]
114. Lim, S.; Akther, N.; Tran, V.H.; Bae, T.-H.; Phuntsho, S.; Merenda, A.; Dumée, L.F.; Shon, H.K. Covalent organic framework incorporated outer-selective hollow fiber thin-film nanocomposite membranes for osmotically driven desalination. *Desalination* **2020**, *485*, 114461. [[CrossRef](#)]
115. Wang, R.; Li, C.; Li, Q.; Zhang, S.; Lv, F.; Yan, Z. Electrospinning fabrication of covalent organic framework composite nanofibers for pipette tip solid phase extraction of tetracycline antibiotics in grass carp and duck. *J. Chromatogr. A* **2020**, *1622*, 461098. [[CrossRef](#)] [[PubMed](#)]
116. Zhang, S.; Yang, Q.; Li, Z.; Wang, W.; Wang, C.; Wang, Z. Covalent organic frameworks as a novel fiber coating for solid-phase microextraction of volatile benzene homologues. *Anal. Bioanal. Chem.* **2017**, *409*, 3429–3439. [[CrossRef](#)] [[PubMed](#)]
117. Wang, Z.; Wu, Z.; Zhang, Y.; Meng, J. Hyperbranched-polyol-tethered poly (amic acid) electrospun nanofiber membrane with ultrahigh adsorption capacity for boron removal. *Appl. Surf. Sci.* **2017**, *402*, 21–30. [[CrossRef](#)]
118. Zhao, R.; Li, X.; Sun, B.; Li, Y.; Li, Y.; Yang, R.; Wang, C. Branched polyethylenimine grafted electrospun polyacrylonitrile fiber membrane: A Novel and Effective Adsorbent for Cr(VI) Remediation in Wastewater. *J. Mater. Chem. A* **2017**, *5*, 1133–1144. [[CrossRef](#)]
119. Gao, H.; He, W.; Zhao, Y.-B.; Opris, D.M.; Xu, G.; Wang, J. Electret mechanisms and kinetics of electrospun nanofiber membranes and lifetime in filtration applications in comparison with corona-charged membranes. *J. Memb. Sci.* **2020**, *600*, 117879. [[CrossRef](#)]
120. Wu, X.-Q.; Wu, X.; Wang, T.Y.; Zhao, L.; Truong, Y.B.; Ng, D.; Zheng, Y.-M.; Xie, Z. Omniphobic surface modification of electrospun nanofiber membrane via vapor deposition for enhanced anti-wetting property in membrane distillation. *J. Memb. Sci.* **2020**, *606*, 118075. [[CrossRef](#)]
121. Liu, C.; Li, X.; Liu, T.; Liu, Z.; Li, N.; Zhang, Y.; Xiao, C.; Feng, X. Microporous CA/PVDF membranes based on electrospun nanofibers with controlled crosslinking induced by solvent vapor. *J. Memb. Sci.* **2016**, *512*, 1–12. [[CrossRef](#)]

122. Su, Q.; Zhang, J.; Zhang, L.-Z. Fouling resistance improvement with a new superhydrophobic electrospun PVDF membrane for seawater desalination. *Desalination* **2020**, *476*, 114246. [[CrossRef](#)]
123. Doan, H.N.; Phong Vo, P.; Hayashi, K.; Kinashi, K.; Sakai, W.; Tsutsumi, N. Recycled PET as a PDMS-Functionalized electrospun fibrous membrane for oil-water separation. *J. Environ. Chem. Eng.* **2020**, *8*, 103921. [[CrossRef](#)]
124. Ursino, C.; Di Nicolò, E.; Gabriele, B.; Criscuoli, A.; Figoli, A. Development of a novel perfluoropolyether (PFPE) hydrophobic/hydrophilic coated membranes for water treatment. *J. Memb. Sci.* **2019**, *581*, 58–71. [[CrossRef](#)]
125. Yang, H.C.; Xie, Y.; Hou, J.; Cheetham, A.K.; Chen, V.; Darling, S.B. Janus Membranes: Creating Asymmetry for Energy Efficiency. *Adv. Mater.* **2018**, *30*, 1801495. [[CrossRef](#)]
126. Woo, Y.C.; Tijing, L.D.; Park, M.J.; Yao, M.; Choi, J.-S.; Lee, S.; Kim, S.-H.; An, K.-J.; Shon, H.K. Electrospun dual-layer nonwoven membrane for desalination by air gap membrane distillation. *Desalination* **2017**, *403*, 187–198. [[CrossRef](#)]
127. Essalhi, M.; Khayet, M.; Tesfalidet, S.; Alsultan, M.; Tavajohi, N. Desalination by direct contact membrane distillation using mixed matrix electrospun nanofibrous membranes with carbon-based nanofillers: A Strategic Improvement. *Chem. Eng. J.* **2021**, *426*, 131316. [[CrossRef](#)]
128. An, X.; Bai, Y.; Xu, G.; Xie, B.; Hu, Y. Fabrication of interweaving hierarchical fibrous composite (iHFC) membranes for high-flux and robust direct contact membrane distillation. *Desalination* **2020**, *477*, 114264. [[CrossRef](#)]
129. Khayet, M.; Garcia-Payo, M.C.; Garcia-Fernandez, L.; Contreras-Martinez, J. Dual-layered electrospun nanofibrous membranes for membrane distillation. *Desalination* **2018**, *426*, 174–184. [[CrossRef](#)]
130. Hou, D.; Ding, C.; Li, K.; Lin, D.; Wang, D.; Wang, J. A novel dual-layer composite membrane with underwater-superoleophobic/hydrophobic asymmetric wettability for robust oil-fouling resistance in membrane distillation desalination. *Desalination* **2018**, *428*, 240–249. [[CrossRef](#)]
131. Pornea, A.M.; Puguan, J.M.C.; Deonikar, V.G.; Kim, H. Robust Janus nanocomposite membrane with opposing surface wettability for selective oil-water separation. *Sep. Purif. Technol.* **2020**, *236*, 116297. [[CrossRef](#)]
132. Yan, K.K.; Jiao, L.; Lin, S.; Ji, X.; Lu, Y.; Zhang, L. Superhydrophobic electrospun nanofiber membrane coated by carbon nanotubes network for membrane distillation. *Desalination* **2018**, *437*, 26–33. [[CrossRef](#)]
133. Jiang, Y.; Hou, J.; Xu, J.; Shan, B. Switchable oil/water separation with efficient and robust Janus nanofiber membranes. *Carbon* **2017**, *115*, 477–485. [[CrossRef](#)]
134. Jia, W.; Kharraz, J.A.; Sun, J.; An, A.K. Hierarchical Janus membrane via a sequential electro spray coating method with wetting and fouling resistance for membrane distillation. *Desalination* **2021**, *520*, 115313. [[CrossRef](#)]
135. Guo, J.; Deka, B.J.; Wong, P.W.; Sun, J.; An, A.K. Fabrication of robust green superhydrophobic hybrid nanofiber-nanosphere membrane for membrane distillation. *Desalination* **2021**, *520*, 115314. [[CrossRef](#)]
136. Huang, M.; Tu, H.; Chen, J.; Liu, R.; Liang, Z.; Jiang, L.; Shi, X.; Du, Y.; Deng, H. Chitosan-rectorite nanospheres embedded aminated polyacrylonitrile nanofibers via shoulder-to-shoulder electrospinning and electro spraying for enhanced heavy metal removal. *Appl. Surf. Sci.* **2018**, *437*, 294–303. [[CrossRef](#)]
137. Guo, J.-W.; Wang, C.-F.; Chen, S.-H.; Lai, J.Y.; Lu, C.-H.; Chen, J.-K. Highly efficient self-cleaning of heavy polyelectrolyte coated electrospun polyacrylonitrile nanofibrous membrane for separation of oil/water emulsions with intermittent pressure. *Sep. Purif. Technol.* **2020**, *234*, 116106. [[CrossRef](#)]
138. Chowdhury, M.R.; Huang, L.; McCutcheon, J.R. Thin Film Composite Membranes for Forward Osmosis Supported by Commercial Nanofiber Nonwovens. *Ind. Eng. Chem. Res.* **2017**, *56*, 1057–1063. [[CrossRef](#)]
139. Shen, L.; Wang, F.; Tian, L.; Zhang, X.; Ding, C.; Wang, Y. High-performance thin-film composite membranes with surface functionalization by organic phosphonic acids. *J. Memb. Sci.* **2018**, *563*, 284–297. [[CrossRef](#)]
140. Jiao, L.; Yan, K.; Wang, J.; Lin, S.; Li, G.; Bi, F.; Zhang, L. Low surface energy nanofibrous membrane for enhanced wetting resistance in membrane distillation process. *Desalination* **2020**, *476*, 114210. [[CrossRef](#)]
141. Löffler, F.B.; Altermann, F.J.; Bucharsky, E.C.; Schell, K.G.; Litter, M.I. Morphological characterization and photocatalytic efficiency measurements of pure silica transparent openell sponges coated with TiO₂. *Int. J. Appl. Ceram. Tec.* **2020**, *17*, 1930–1939. [[CrossRef](#)]
142. Zhao, R.; Li, X.; Sun, B.; Ji, H.; Wang, C. Diethylenetriamine-assisted synthesis of amino-rich hydrothermal carbon-coated electrospun polyacrylonitrile fiber adsorbents for the removal of Cr(VI) and 2,4-dichlorophenoxyacetic acid. *J. Colloid Interface Sci.* **2017**, *487*, 297–309. [[CrossRef](#)] [[PubMed](#)]
143. Ren, L.-F.; Xia, F.; Chen, V.; Shao, J.; Chen, R.; He, Y. TiO₂-FTCS modified superhydrophobic PVDF electrospun nanofibrous membrane for desalination by direct contact membrane distillation. *Desalination* **2017**, *423*, 1–11. [[CrossRef](#)]
144. Vanangamudi, A.; Dumeé, L.F.; Des Ligneris, E.; Duke, M.; Yang, X. Thermo-responsive nanofibrous composite membranes for efficient self-cleaning of protein foulants. *J. Memb. Sci.* **2019**, *574*, 309–317. [[CrossRef](#)]
145. Al-Attabi, R.; Morsi, Y.; Schutz, J.A.; Dumeé, L.F. One-pot synthesis of catalytic molybdenum based nanocomposite nano-fiber membranes for aerosol air remediation. *Sci. Total Environ.* **2019**, *647*, 725–733. [[CrossRef](#)] [[PubMed](#)]
146. Tian, E.; Wang, X.; Zhao, Y.; Ren, Y. Middle support layer formation and structure in relation to performance of three-tier thin film composite forward osmosis membrane. *Desalination* **2017**, *421*, 190–201. [[CrossRef](#)]
147. Shokrollahzadeh, S.; Tajik, S. Fabrication of thin film composite forward osmosis membrane using electrospun polysulfone/polyacrylonitrile blend nanofibers as porous substrate. *Desalination* **2018**, *425*, 68–76. [[CrossRef](#)]

148. Park, M.J.; Gonzales, R.R.; Abdel-Wahab, A.; Phuntsho, S.; Shon, H.K. Hydrophilic polyvinyl alcohol coating on hydrophobic electrospun nanofiber membrane for high performance thin film composite forward osmosis membrane. *Desalination* **2018**, *426*, 50–59. [[CrossRef](#)]
149. Mahdavi, H.; Moslehi, M. A new thin film composite nanofiltration membrane based on PET nanofiber support and polyamide top layer: Preparation and Characterization. *J. Polym. Res.* **2016**, *23*, 257. [[CrossRef](#)]
150. Kaur, G.A.; Shandilya, M.; Rana, P.; Thakur, S.; Uniyal, P. Modification of structural and magnetic properties of $\text{Co}_{0.5}\text{Ni}_{0.5}\text{Fe}_2\text{O}_4$ nanoparticles embedded Polyvinylidene Fluoride nanofiber membrane via electrospinning method. *Nano-Struct. Nano Objects* **2020**, *22*, 100428. [[CrossRef](#)]